

Supplementary information

Targeted glycan degradation potentiates the anticancer immune response *in vivo*

In the format provided by the
authors and unedited

Supplementary Information

Targeted glycan degradation overcomes glyco-immune checkpoints and potentiates the anticancer immune response *in vivo*

Melissa A. Gray, Michal A. Stanczak, Natália R. Mantuano, Han Xiao, Johan F. A. Pijnenborg, Stacy A. Malaker, Caitlyn L. Miller, Payton A. Weidenbacher, Julia T. Tanzo, Green Ahn, Elliot C. Woods, Heinz Läubli, Carolyn R. Bertozzi

Correspondence to: bertozzi@stanford.edu

This PDF file includes:

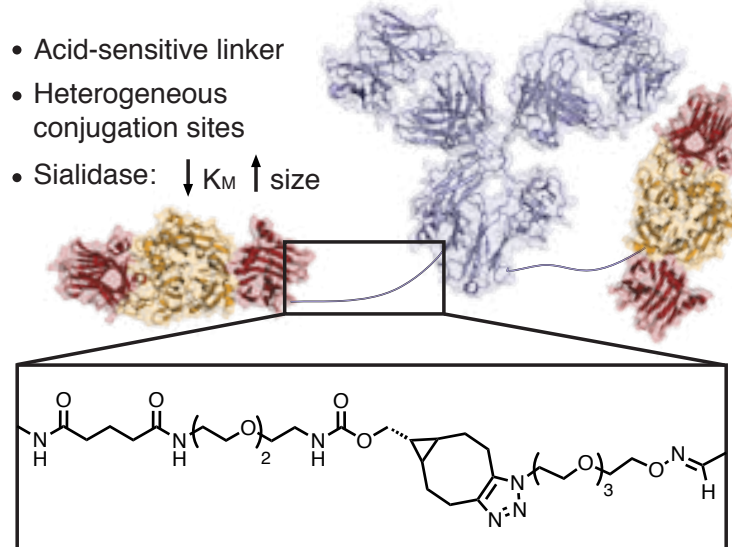
Supplementary Table 1
Supplementary Figures 1-22
Supplementary Note 1
Supplementary Note 2

Supplementary Table 1. Antibody and lectin reagent information and concentrations

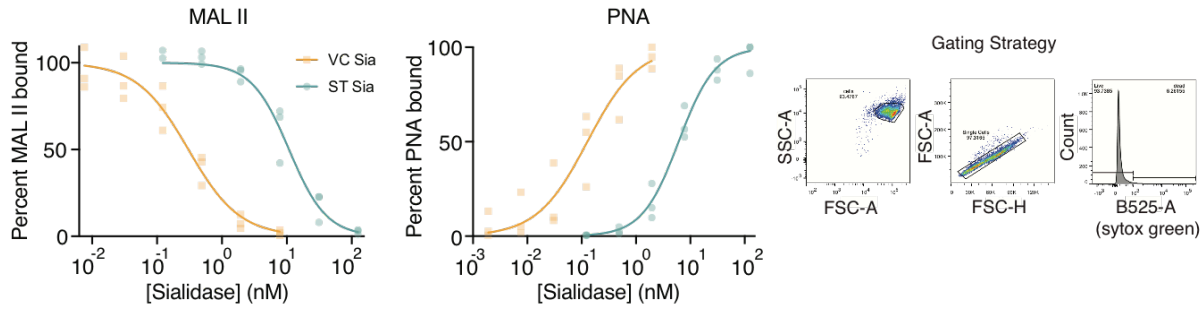
Antibody or Lectin	Source (#)	Usage, dilution
Alexa Fluor® 647 anti-human Her2 antibody	Biolegend (324412)	FC, 1:100
FITC Conjugated <i>Sambucus nigra</i> (Elderberry Bark) -SNA-I-, 1mg	EY Laboratories (F-6802-1)	FC, 1:100
Siglec-7-Fc Chimera protein	R&D Systems (1138-SL-050)	FC, 1:50
Siglec-9-Fc Chimera protein	R&D Systems (1139-SL-050)	FC, 1:50
Siglec-F-Fc Chimera protein	R&D Systems (1706-SF-050)	FC, 1:50
Alexa Fluor® 488 AffiniPure Goat Anti-Human IgG, Fcγ fragment specific	Jackson ImmunoResearch (109-545-008)	FC, 1:375
PE/Dazzle™ 594 anti-mouse CD3 Antibody	Biolegend (100246)	FC, 1:100
Brilliant Violet 605™ anti-mouse CD4 antibody	Biolegend (100548)	FC, 1:100
Brilliant Violet 785™ anti-mouse CD8a Antibody	Biolegend (100750)	FC, 1:100
Alexa Fluor® 488 Rat Anti-CD11b	BD Pharmingen (557672)	FC, 1:100
PE-Cy™7 Hamster Anti-Mouse CD11c	BD Biosciences (561022)	FC, 1:100
BV421 Rat Anti-Mouse CD19	BD Pharmingen (562701)	FC, 1:100
FITC anti-mouse CD25 Antibody	Biolegend (102005)	FC, 1:100
CD45 Monoclonal Antibody (30-F11), PerCP-Cyanine5.5	eBioscience (45-0451-82)	FC, 1:100 (FC, 1:400: Supp. Fig. 31)
APC anti-mouse CD69 Antibody	Biolegend (104514)	FC, 1:100
APC anti-mouse CD206 (MMR) Antibody	Biolegend (141708)	FC, 1:50
PE Rat Anti-Mouse CD335 (NKP46) Clone 29A1.4	BD (560757)	FC, 1:50
Alexa Fluor® 647 anti-mouse/rat/human FOXP3 Antibody	Biolegend (320014)	FC, 1:100
APC/Cyanine7 anti-mouse I-A/I-E Antibody	Biolegend (107628)	FC, 1:200
Brilliant Violet 421™ anti-mouse F4/80 Antibody	Biolegend (123132)	FC, 1:100
FITC Mouse anti-Human Granzyme B Clone GB11	BD (560211)	FC, 1:100
PE/Cy7 Streptavidin	Biolegend (405206)	FC, 1:400
Biotinylated Concanavalin A (Con A)	Vector Labs (B-1005)	FC, 10 µg/mL
Biotinylated Peanut Agglutinin (PNA)	Vector Labs (B-1075)	FC, 10 µg/mL IHC: 20 µg/mL
Biotinylated Maackia Amurensis Lectin II (MALII)	Vector Labs (B-1265)	FC, 10 µg/mL IHC: 20 µg/mL
Biotinylated <i>Sambucus Nigra</i> Lectin (SNA, EBL)	Vector Labs (B-1305)	FC, 10 µg/mL IHC: 20 µg/mL
Streptavidin Streptavidin, Alexa Fluor™ 647 conjugate	Thermo (S21374)	FC: 2 µg/mL IHC: 15 µg/mL
APC anti-human CD328 (Siglec-7)	BioLegend (339206)	FC, 1:10
APC Mouse IgG1, κ Isotype Ctrl	BioLegend (400122)	FC, 1:10
APC anti-human Siglec-9	BioLegend (351506)	FC, 1:10
FITC anti-human CD3	BioLegend (300306)	FC, 1:10
PE anti-human TCR γ/δ	BioLegend (331210)	FC, 1:10
Live/Dead Fixable Violet Dead Cell Stain kit	Thermo Fisher Scientific (L34963)	FC: 1:1000
PE/Cy7 anti-human CD16	BioLegend (302016)	FC, 1:10
UltraComp eBeads™ Compensation Beads	Thermo Fisher Scientific (01-2222-42)	-----

CD314 (NKG2D) Monoclonal Antibody APC	eBioscience™ (14-5879-82)	FC, 1:10
APC/Cyanine7 anti-mouse CD19 Antibody	Biolegend (115529)	FC, 1:200
PE anti-mouse CD3ε Antibody	Biolegend (100308)	FC, 1:200
NK1.1 Monoclonal Antibody (PK136), PE-Cyanine7	eBioscience (25-5941-82)	FC, 1:200
PE anti-Siglec-E Antibody	Biolegend (677104)	FC, 1:50
FITC anti-mouse/human CD11b Antibody	Biolegend (101206)	FC, 1:300
BV786 Rat Anti-Mouse CD4	BD Horizon (563331)	FC, 1:100
Brilliant Violet 605™ anti-mouse CD8a Antibody	Biolegend (100744)	FC, 1:100
Zombie UV™ Fixable Viability Kit	Biolegend (423108)	FC, 1:200

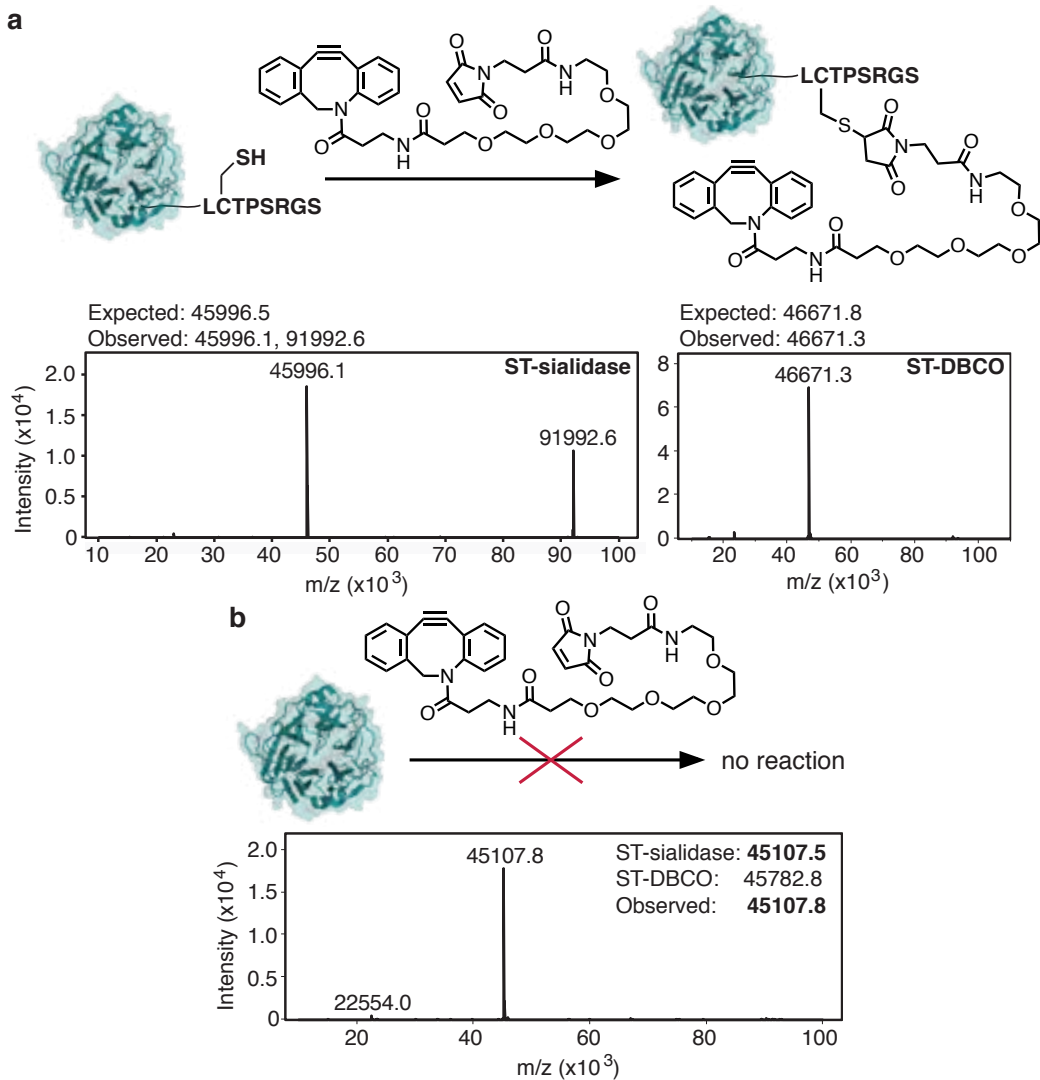
T-Sia version 1



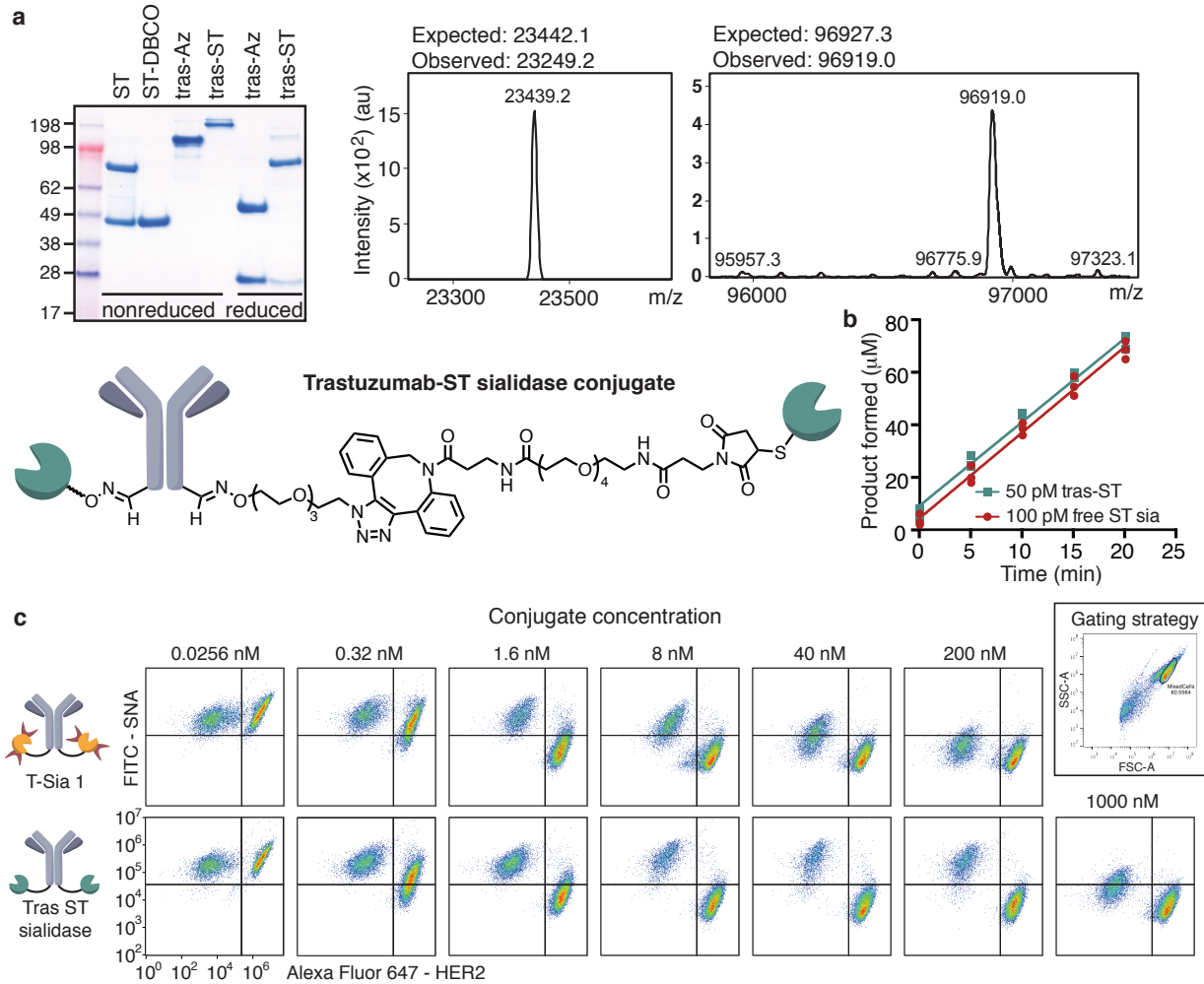
Supplementary Fig. 1. Chemistry of T-Sia version 1 linker previously reported²². T-Sia 1 was constructed by chemical conjugation of VC sialidase to a site near the C-terminus of each trastuzumab heavy chain²². SMARTag technology³⁰ was employed to introduce site-specifically an aldehyde group onto trastuzumab's heavy chains, which was then conjugated via oxime formation to an azide-terminated PEG linker. In parallel, a cyclooctyne group was incorporated onto VC sialidase through non-specific acylation of the enzyme's lysine residues. The two proteins were finally joined by copper-free click chemistry³².



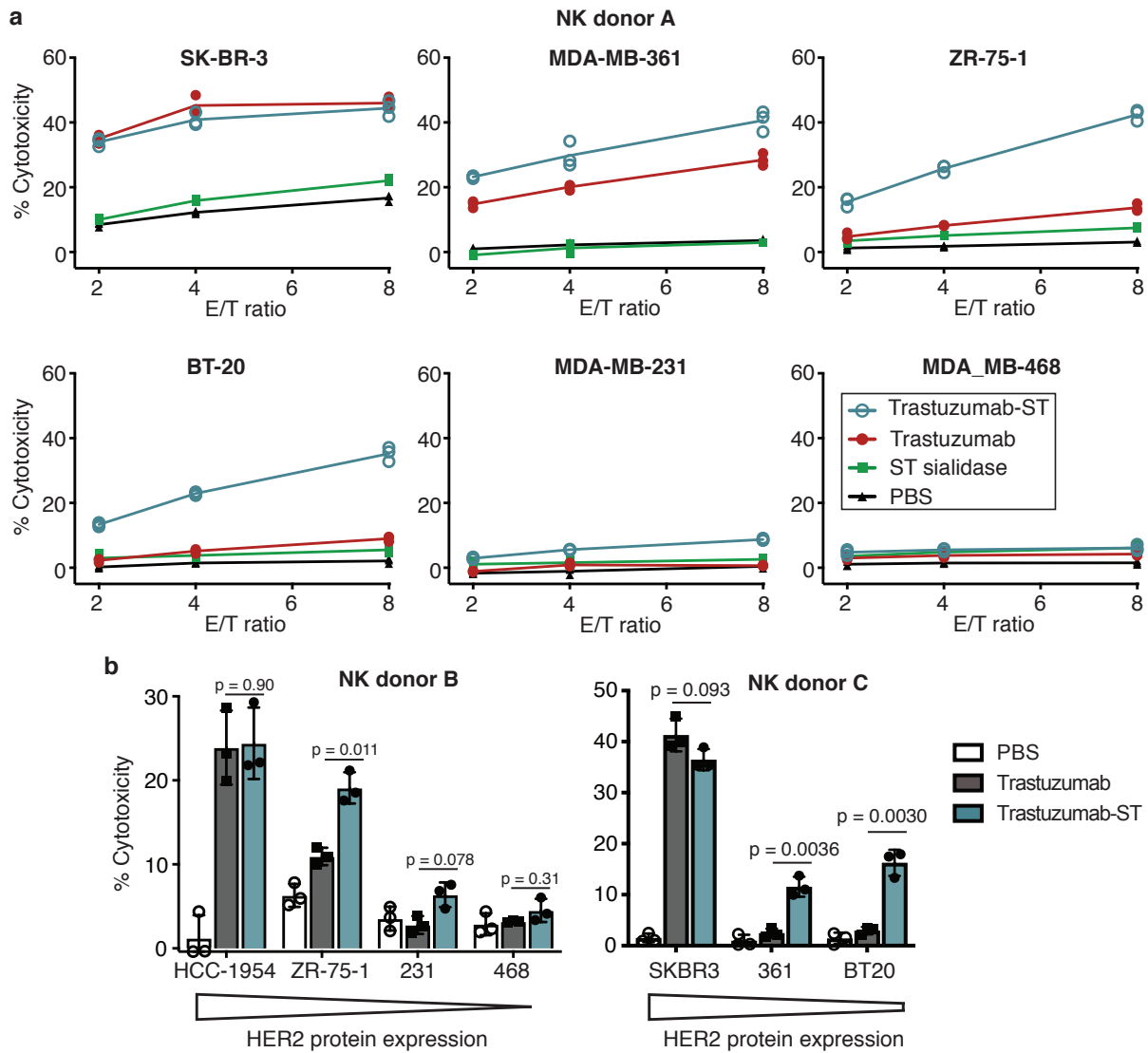
Supplementary Fig. 2. Free *Vibrio cholerae* sialidase destroys sialoglycans at lower concentrations than free *Salmonella typhimurium* sialidase, demonstrating larger off-target effects. HER2⁺ EMT6 cells were treated with VC or ST sialidase at various concentrations and sialoglycan depletion was detected by biotinylated Maackia Amurensis Lectin II (MALII), which preferentially binds sialic acid in an (α -2,3) linkage, and Peanut Agglutinin (PNA), which binds preferentially to the T-antigen, a galactosyl (β -1,3) N-acetylgalactosamine structure that is exposed upon sialic acid removal. Sialidase treatment concentrations from n=3 independent experiments (all data points shown) are plotted on a log scale and fitted to a four-parameter variable slope, where ST sialidase consistently has EC₅₀ values 10-50 fold higher than VC sialidase. Flow cytometry gating for the cell population is shown on the right: cells were first gated for size using the SSC-A/FSC-A gates, then single cells were selected (FSC-A/FSC-H), followed by gating on living cells negative for sytox green.



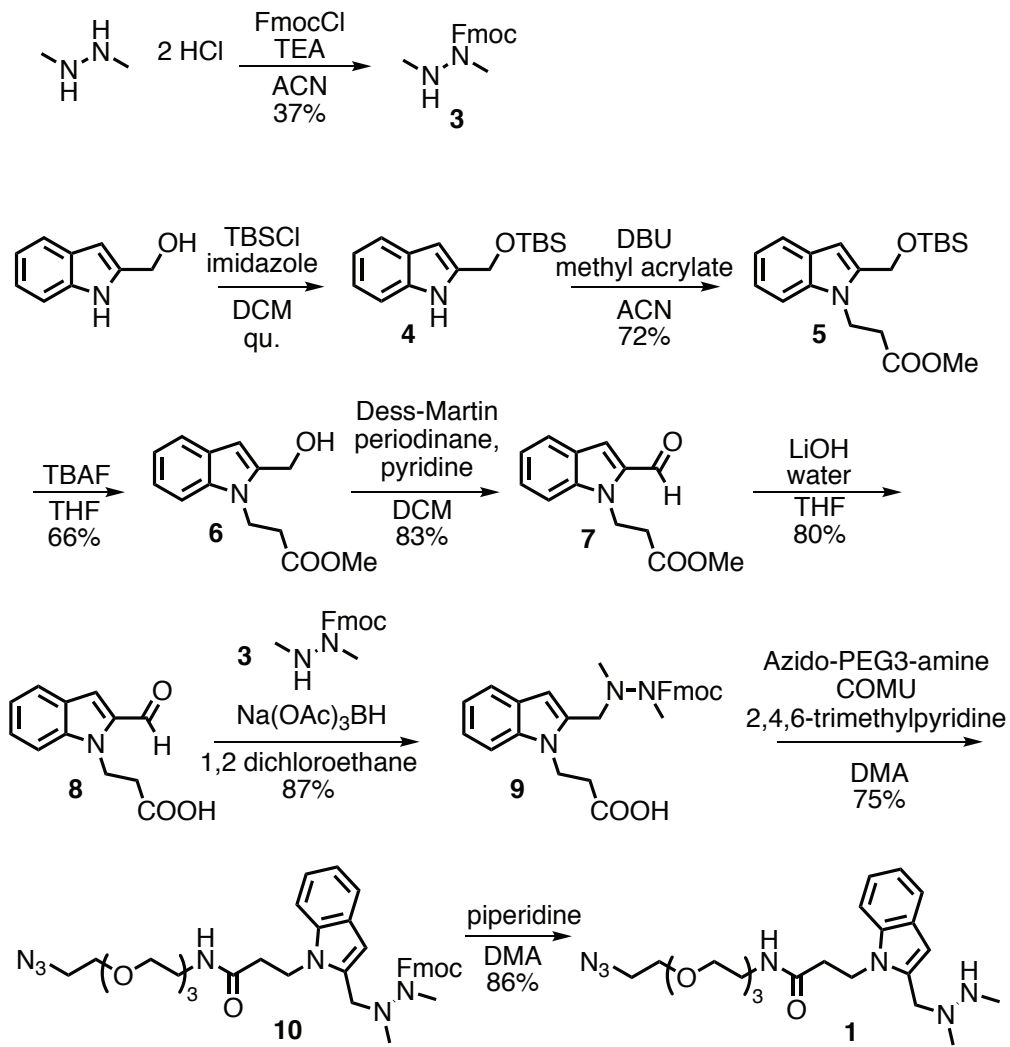
Supplementary Fig. 3. Maleimide-PEG4-DBCO was site-specifically incorporated at the ST sialidase C-terminus in the synthesis of the first trastuzumab-ST conjugate. **a**, ST sialidase expressed with the amino acid sequence SLCTPSRGS at the C-terminus was incubated with 20 mM TCEP at 4 °C in the dark for 10 min, then 20 equiv. maleimide-PEG4-DBCO was added and the reaction was rotated overnight at 4 °C and purified by size exclusion chromatography. Expected m/z shift was observed by ESI-TOF MS for addition of 1 DBCO molecule; no peaks were observed for m/z corresponding to multiple maleimide-PEG4-DBCO additions. **b**, A representative control reaction (from n=3 independently performed reactions) with ST sialidase that lacked the C-terminal peptide tag on sialidase resulted in no observable addition of DBCO to endogenous cysteine residues ESI-TOF-MS.



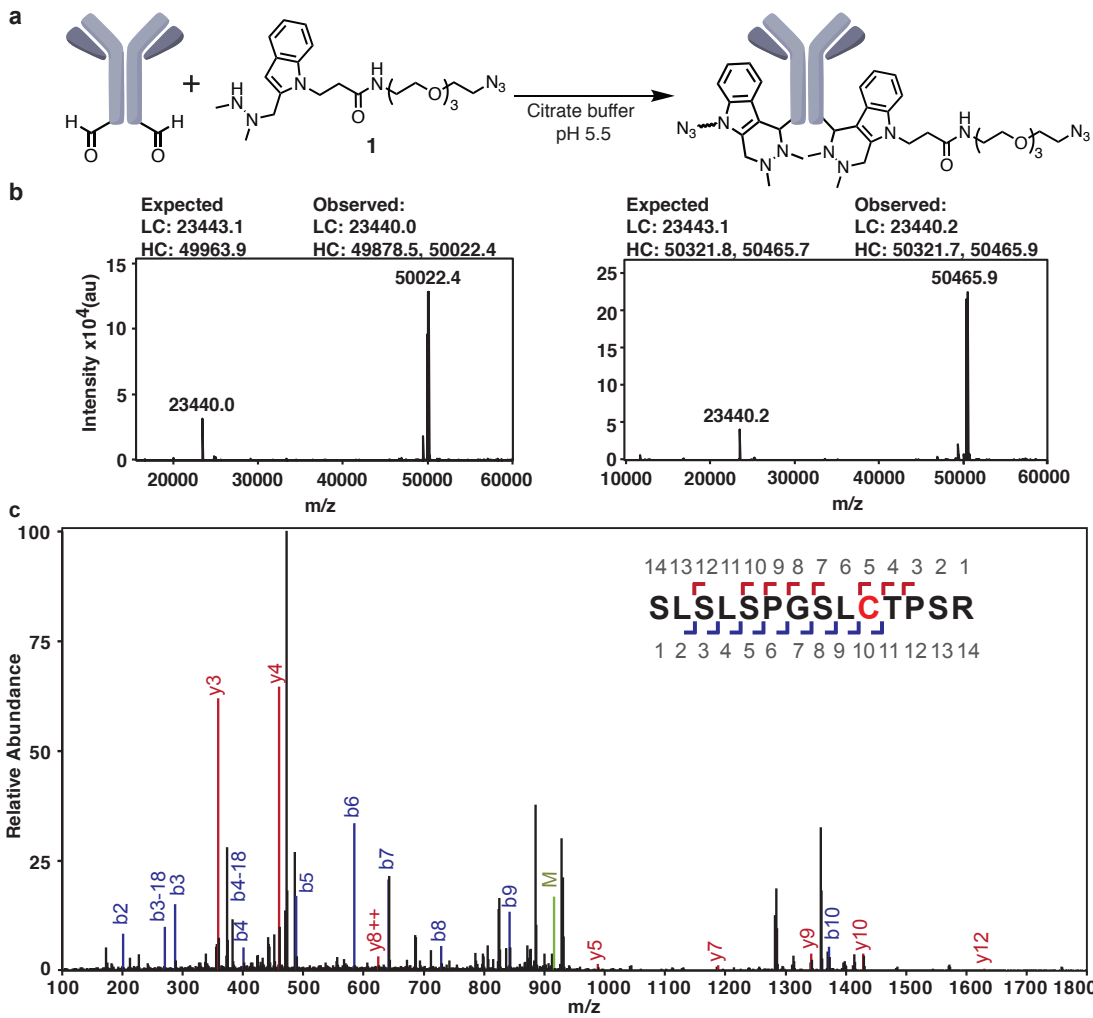
Supplementary Fig. 4. Characterization of the preliminary ST sialidase-trastuzumab conjugate including selective sialoglycan degradation of a HER2+ breast cancer cell line. **a**, Left: PAGE-SDS gel of ST sialidase (ST), ST Sialidase modified with maleimide-PEG4-DBCO (ST-DBCO), trastuzumab-oxime-azide (tras-Az), and trastuzumab ST sialidase conjugate (tras-ST). Right: ESI-TOF mass spectra of the light and heavy chains of tras-ST demonstrating ST sialidase addition selectively to the heavy chain. Below: chemical representation of tras ST. **b**, *In vitro* activity assay of trastuzumab ST sialidase conjugate (tras-ST) (50 pM) with an Antibody/Enzyme ratio =2, and ST sialidase (100 pM). Release of the fluorescent 4-methylumbelliferyl from the 4-MUNANA fluorogenic probe was detected by plate reader (n=3, all data points shown, fit to linear regression). **c**, Representative of n=3 flow cytometry plots of the averaged data shown in Fig. 2C. *Note: the SNA lectin is highly toxic to cells and kills cells it binds to selectively, this creates a depleted cell count ratio when one cell line is SNA-negative and one cell line is SNA-positive (see tras ST sialidase-treated samples at 8 and 40 nM, as an example), in future we would recommend experimenters fix their cells after desialylation and prior to SNA binding to avoid this effect.



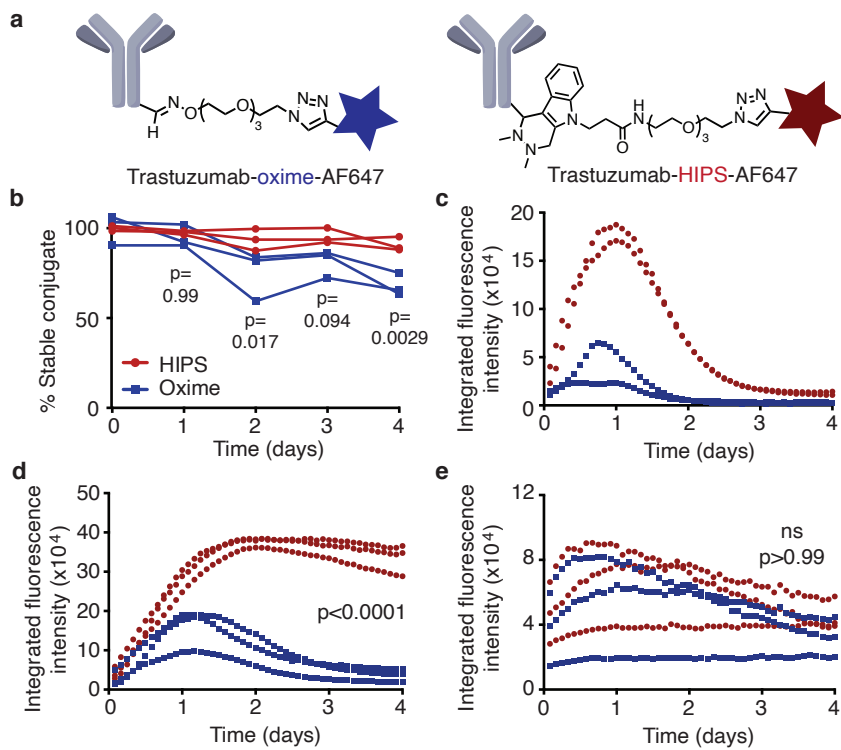
Supplementary Fig. 5. Trastuzumab-ST enhances NK cell-mediated ADCC against many HER2⁺ cell lines using human NK cells from multiple donors; this effect increases with increasing effector to target cell (E/T) ratios. **a**, Percent cytotoxicity from IL-2 activated NK cell-mediated ADCC against six target breast cancer cell lines at E/T = 2 and E/T = 4 (in addition to the E/T=8 displayed in Fig. 2D). Cells were treated with PBS, ST sialidase (20 nM), trastuzumab (10 nM), or trastuzumab-ST sialidase (trastuzumab-ST, 10 nM). The mean is shown as a line connecting the different E/T ratios for n=3* experimental replicates of the percent cytotoxicity detected with the LDH release method after 4 h (*n=2 for MDA-MB-361 PBS E/T=8). **b**, IL-2 activated NK cell-mediated ADCC from two additional biological NK donors on various breast cancer cell lines, E/T=4, mean \pm SD depicted from n=3 experimental replicates, detecting LDH release after 4 h, statistical analysis by multiple two-sided t tests; p-values shown have been corrected for multiple comparisons using the Holm-Sidak method with an alpha of 0.05.



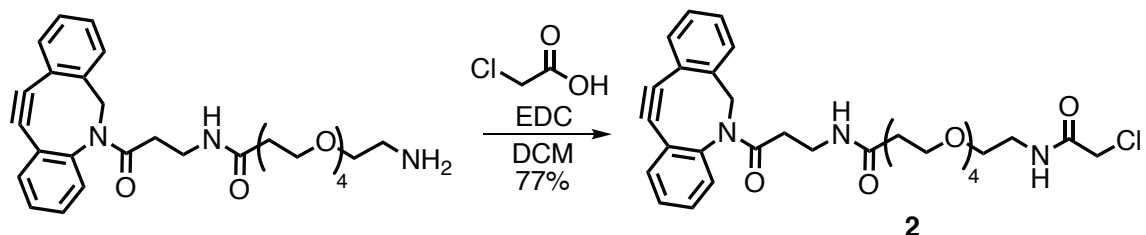
Supplementary Fig. 6. Synthesis of HIPS-azide linker. Synthetic route to HIPS-azide (1) and associated reaction yields. Synthesis of 3-9 was performed as described previously^{27,28}, with a modified purification of compound 9. Synthesis and purification of compounds 9, 10, and 1 are described further in Supplementary Note 2.



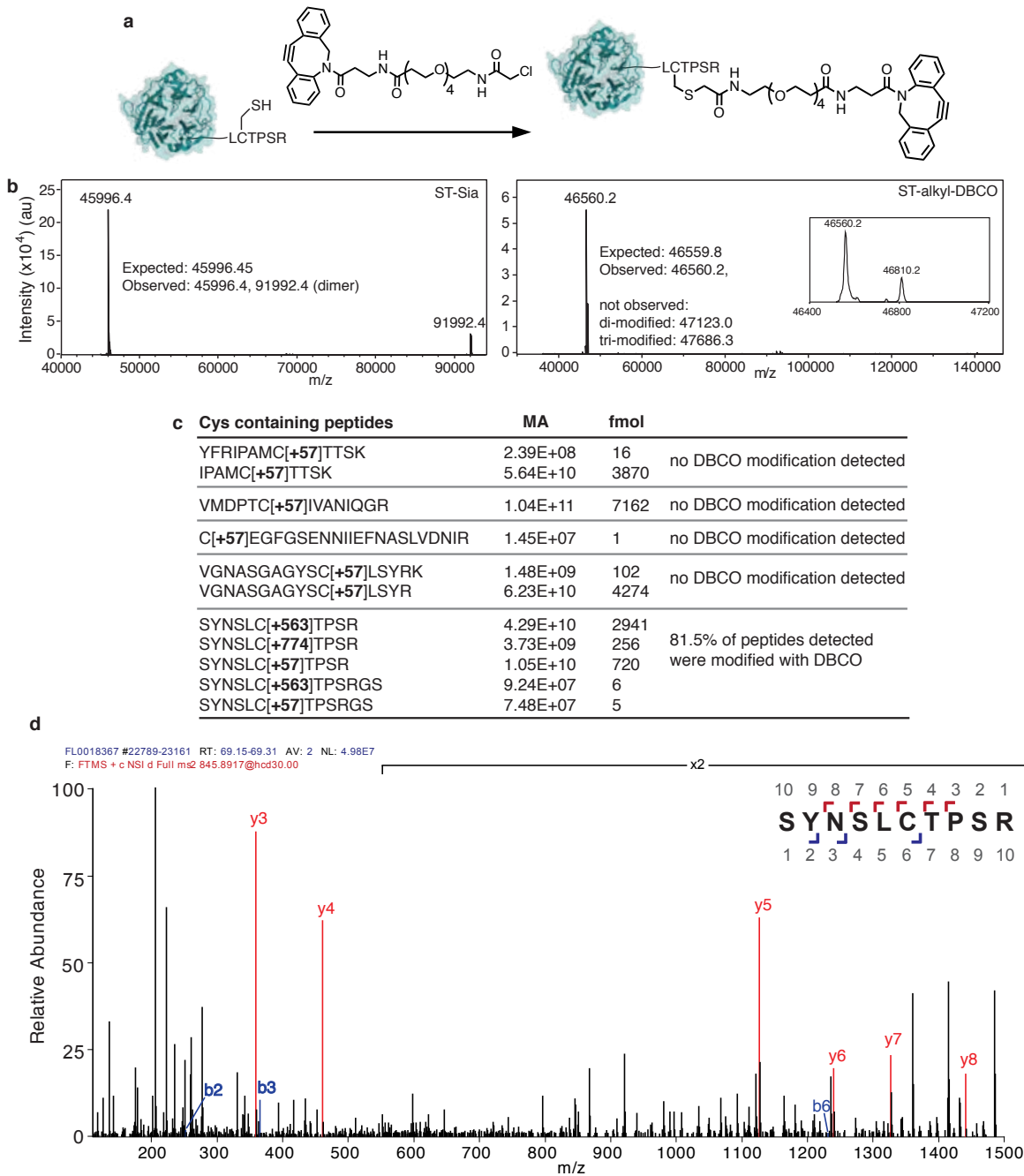
Supplementary Fig. 7. Synthesis and characterization of the site-specific modification of HIPS-azide to the trastuzumab formylglycine residue. **a**, Trastuzumab was synthesized by reacting HIPS-azide (**1**) in DMSO with SMARTag-labeled trastuzumab under acidic conditions in citrate buffer for 24 h at 37 °C shaking. **b**, Representative ESI-TOF mass spectra of reduced antibody chains before and after HIPS conjugation, the addition of HIPS-azide was confirmed for n=3 independently performed reactions at different scales. **c**, Peptide mass spectrum of the trastuzumab heavy-chain C-terminal trypsin digested peptide covalently modified with the HIPS linker; HIPS addition was not detected on other trastuzumab cysteine residue. This data is from n=1 experiment run on the final molecule and is consistent with n=3 other independently run mass spectral characterizations performed during the optimization of the reaction conditions in **a**.



Supplementary Fig. 8. The HIPS linker used to make T-Sia 2 is more stable in serum and bound to living cells than the oxime linker. **a**, Alexa Fluor 647 Alkyne was reacted with trastuzumab-azide antibodies using copper-click chemistry. Trastuzumab-oxime-AF647 contains the oxime bond used in T-Sia 1; Trastuzumab-HIPS-AF647 contains the new HIPS linker. **b**, Trastuzumab-HIPS-647 and trastuzumab-oxime-647 were incubated in human plasma at 37 °C. After two days, there was significantly less trastuzumab-oxime-647 than trastuzumab-HIPS-647. Ordinary two-way ANOVA ($p = 0.036$) with Sidak's multiple comparisons reported below each time point ($\alpha=0.05$); $n=3$ experimental replicates. **c-d**, To determine the conjugates' stabilities on cell surfaces and in endocytic compartments, 50 nM Tras-HIPS-647 and tras-oxime-647 were incubated on the surface of adherent HCC-1954 cells for 1 hour, and then solution was removed and replaced with either **(c)** normal media or **(d)** media containing protease inhibitor. Fluorescence was monitored by IncuCyte and total integrated fluorescence was quantified every 2 h. The HIPS linker fluorescent signal outlasted the oxime linker, and when protease inhibitor was added there was minimal degradation of trastuzumab-HIPS-AF647, while trastuzumab-oxime-647 lost fluorescence from protease-independent cleavage. **e**, Conditions from **(c)** were used on the surface of fixed cells to prevent cellular endocytosis and proteolysis. On dead cells in 10% serum, both chemistries gave similar fluorescence signals over time. Values shown are from $n=2$ **(c)** or $n=3$ **(d,e)** independently performed experimental replicates (averaged from $n=2$ technical replicates each time). P values are reported from an ordinary two-way ANOVA.

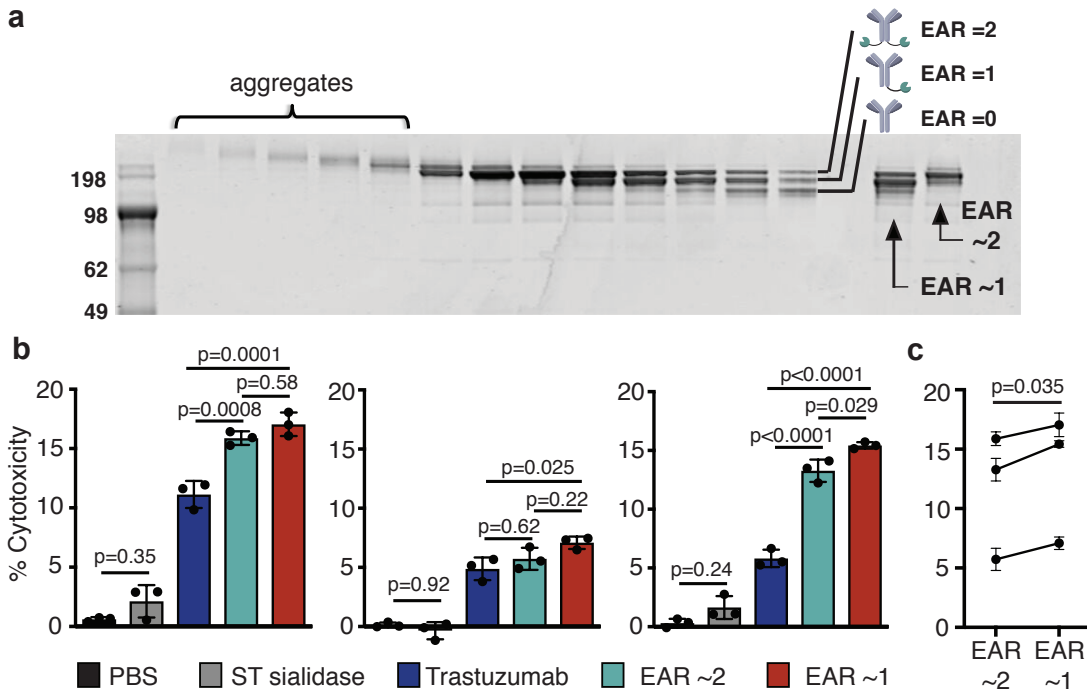


Supplementary Fig. 9. Synthesis of α -chloroacetamide-DBCO (2). DBCO-PEG4-amine was treated with chloroacetic acid in the presence of EDC in DCM to yield α -Chloroacetamide-DBCO (2).

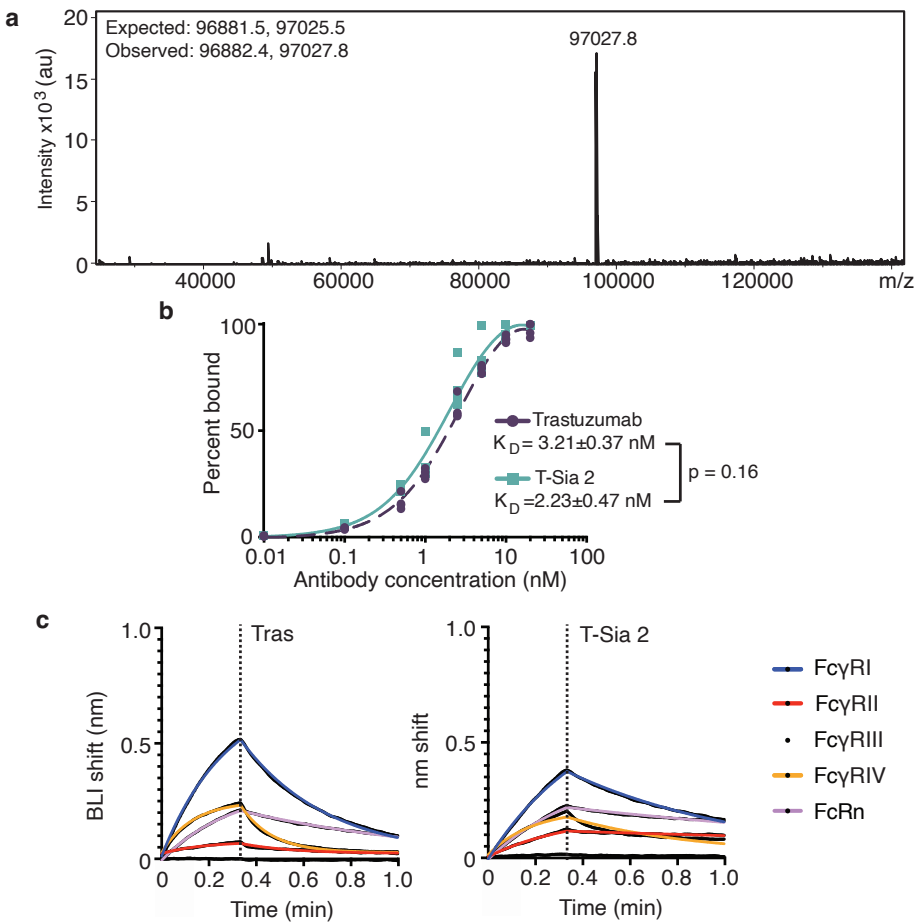


Supplementary Fig. 10. Site-specific conjugation of the α -chloroacetamide-DBCO molecule onto ST sialidase to make ST-DBCO. **a**, α -chloroacetamide-DBCO was conjugated to ST sialidase under mildly reducing and basic conditions (20 mM TCEP in 50 mM ammonium bicarbonate buffer pH 8.3, rotating overnight). **b**, Representative ESI-TOF mass spectrum of sialidase-DBCO, reaction was repeated for n=3 independent reactions at different reaction scales with consistent results. **c**, Summary of results from tryptic ST digestion followed by HCD on the Orbitrap Fusion: all cysteine-containing peptides were detected. Only the cysteine in the C-terminal (SLCTPSR) peptide had a mass shift correlating to α -chloroacetamide-DBCO addition. **d**, MS2

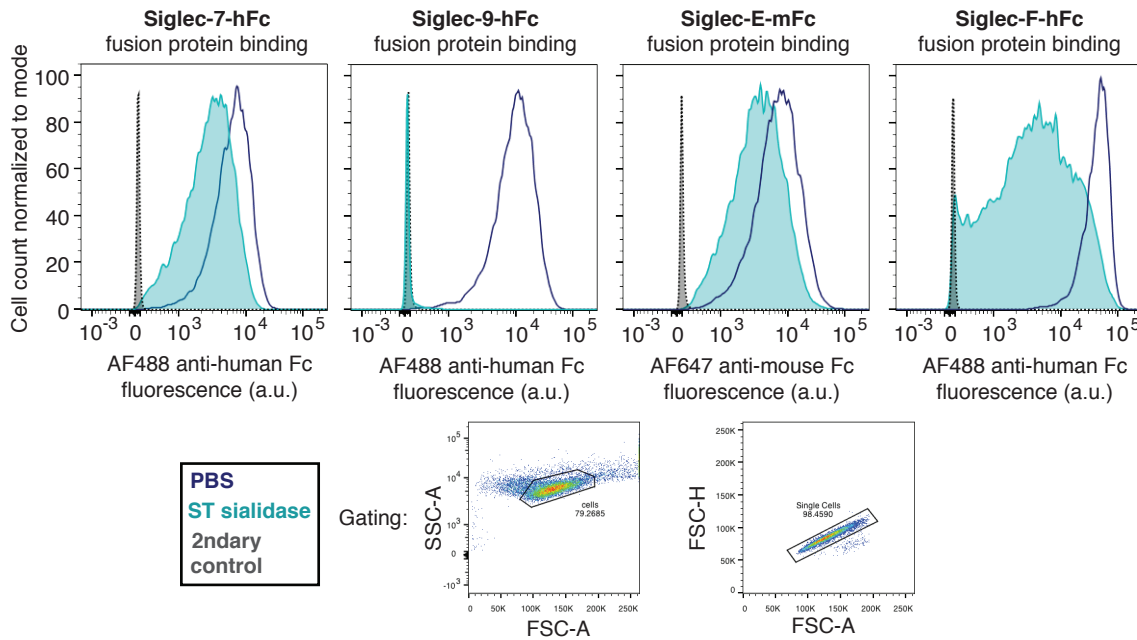
spectrum of the modified SLCTPSR peptide from (**c**). This data is from n=1 experiment run on the final molecule, but is consistent with n=2 other independent mass spectral characterizations performed during the optimization of the reaction conditions in a.



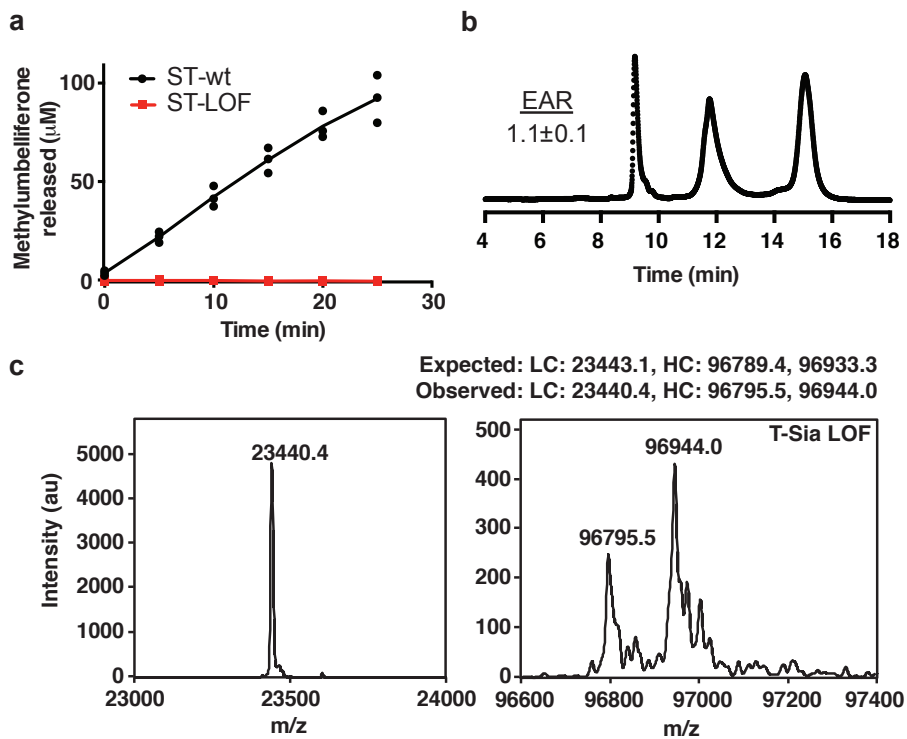
Supplementary Fig. 11. An enzyme/antibody ratio of ~1 demonstrates improved NK cell-mediated ADCC over an enzyme/antibody ratio of ~2. **a**, Representative nonreducing SDS-PAGE gel of purified fractions after size exclusion chromatography of T-Sia 2 separating large aggregates from di-sialidase T-Sia 2, mono-sialidase T-Sia 2, and trastuzumab alone, n=7 size exclusion runs and gels were performed, all very consistent with the above. (Right of gel): two isolated collected fractions with an EAR (Enzyme/Antibody Ratio) ~1 and ~2. **b**, Mean \pm SD of NK cell-mediated ADCC with three different NK cell donors against BT-20 cells treated with PBS, 20 nM of ST sialidase, or 10 nM of trastuzumab, T-Sia EAR ~2, and T-Sia EAR ~1, n=3 experimental replicates for each biological NK cell donor. NK cells were IL-2 treated, followed by and incubation with target BT-20 cells at E/T = 1. Percent cytotoxicity was determined from the LDH release after 8 h, statistical analysis by one way ANOVA with Tukey's multiple comparisons adjusted p-values reported. **c**, Mean \pm SD from ADCC with the three biological NK cell donors shown in (b) reveals a 1.13-fold increase in NK cell-mediated ADCC by EAR~1 over EAR~2, analyzed by a paired two-sided t-test.



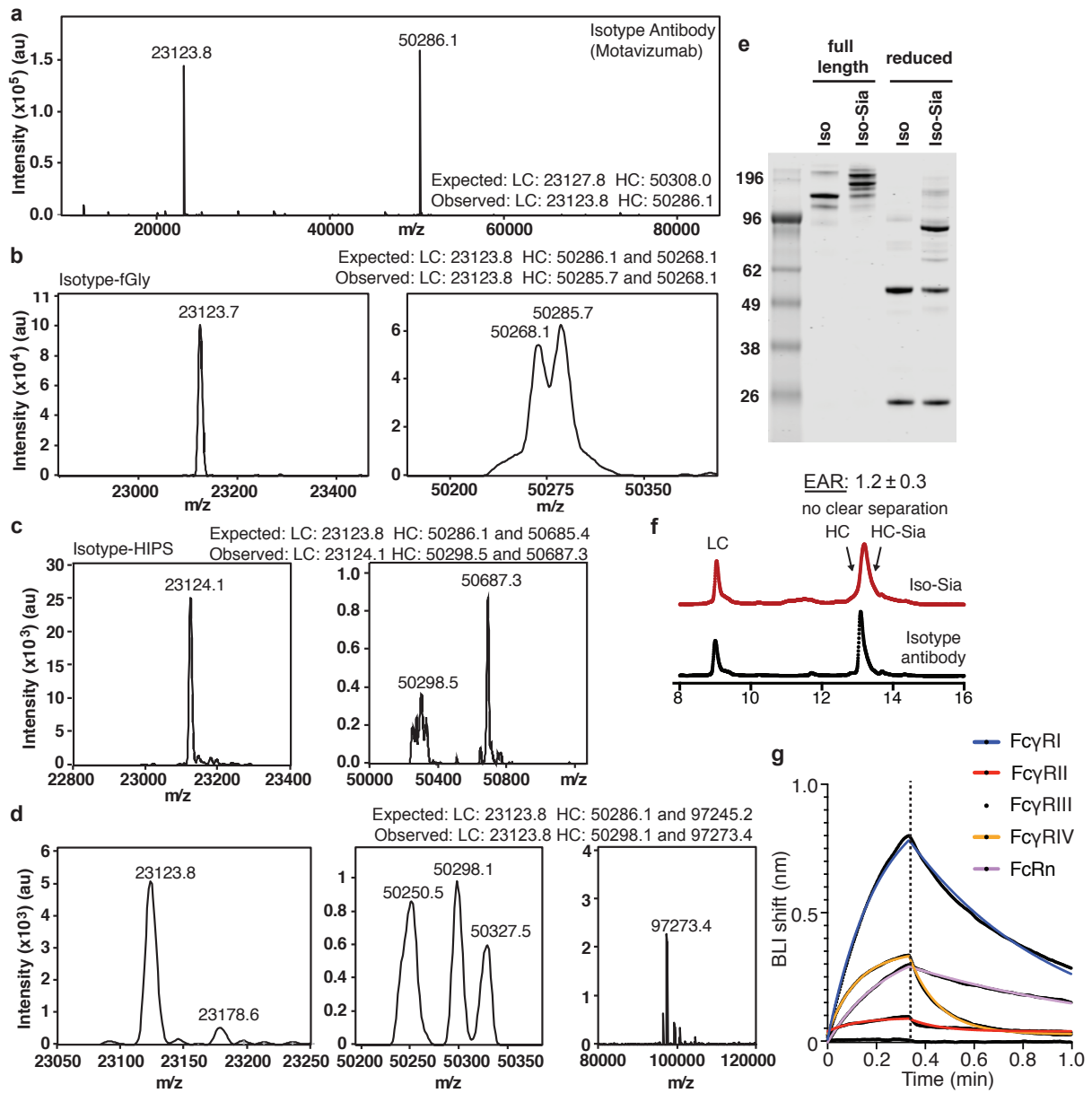
Supplementary Fig. 12. T-Sia 2 maintained sialidase activity and did not significantly alter the binding thermodynamics of trastuzumab alone to HER2+ cells. **a**, ESI-TOF mass spectrum of conjugated sialidase heavy chain. **b**, Flow cytometry assay showing trastuzumab and T-Sia 2 binding curve to SK-BR-3 breast cancer cells, $n=4$ experimental replicates, least-squares one-site total binding curve calculated using GraphPad Prism software. K_D values from the binding curves were not significantly different by two-tailed t test. **c**, Representative binding of trastuzumab (left) and T-Sia 2 (right) to mouse Fc receptors as measured by BLI from $n=2$ independent experiments. Association was monitored for 20 s followed by dissociation for 40 s. Consistent with previously reported human antibody-mFc binding studies, both trastuzumab and T-Sia 2 bind to all mouse Fc receptors except for mouse FcγRIII. The proposed “functional homolog” of hFcγRIII in mice is mFcγRIV - Bruhns, P. Properties of mouse and human IgG receptors and their contribution to disease models. *Blood* **119**, 5640–5650 (2015) – although the sialidase conjugated antibody appears to have a reduced off rate, it is unclear if this would be true on a cell surface.



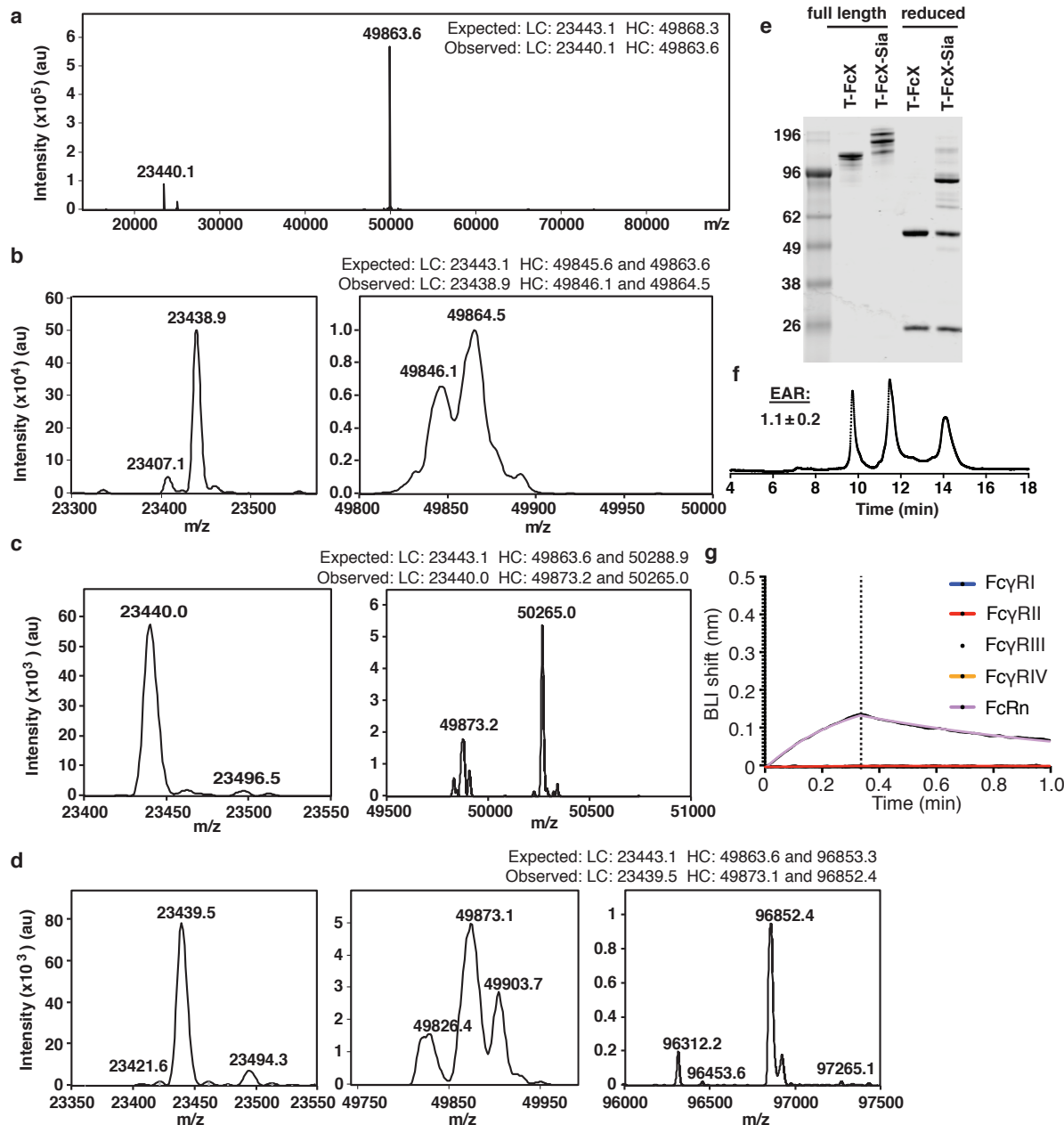
Supplementary Fig. 13. ST sialidase can efficiently cleave Siglec ligands from the mouse EMT6 cancer line. Representative of $n=3$ independently performed flow cytometry experiments of Siglec-Fc binding to EMT6 cancer cells reveals that treatment with high ST sialidase concentration (2 μ M) can reduce human Siglec-7 and -9 and mouse Siglec-E and -F binding to cells. Greater than 12,000 cells are reported on each histogram, normalized to mode. PBS control-treated cells are outlined in dark blue, ST sialidase-treated cells are filled in with teal, and secondary only fluorophore control are in dashed gray. Gating is shown below: cells were first selected by size with the SSC-A and FSC-A gates, then single cells were isolated using the FSC-A and FSC-H.



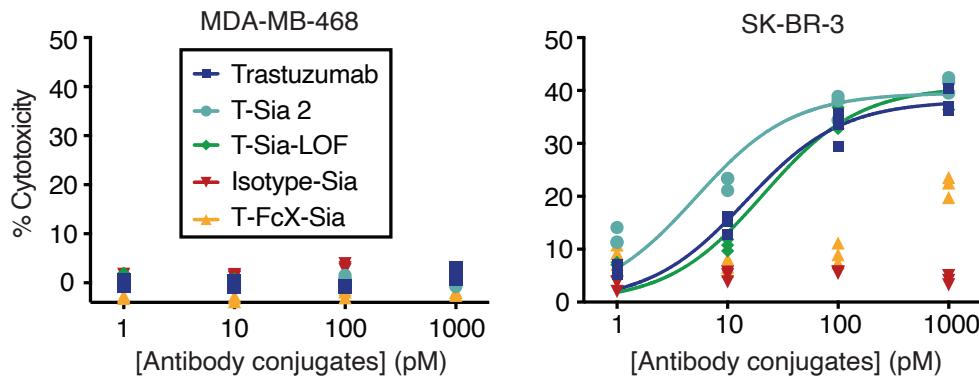
Supplementary Fig. 14. ST-LOF, a single alanine point mutation resulting in decreased ST sialidase activity, was expressed, purified, and conjugated to trastuzumab-HIPS-azide to make T-Sia-LOF. **a**, *In vitro* enzyme activity assay with the fluorogenic substrate 4-MU-NANA comparing the enzymatic activity of ST sialidase vs. ST-LOF sialidase at 75 pM concentrations with 1 mM substrate, n=3 experimental replicates, line connects the mean value at each recorded time point. **b**, Representative (n=3) RP-HPLC trace showing EAR = 1.1 for T-Sia-LOF. **c**, ESI-TOF mass spectrometry revealed unchanged light chain and an increased heavy chain mass indicative of LOF sialidase addition, this reaction was repeated n=3 times at different reaction scales with similar results.



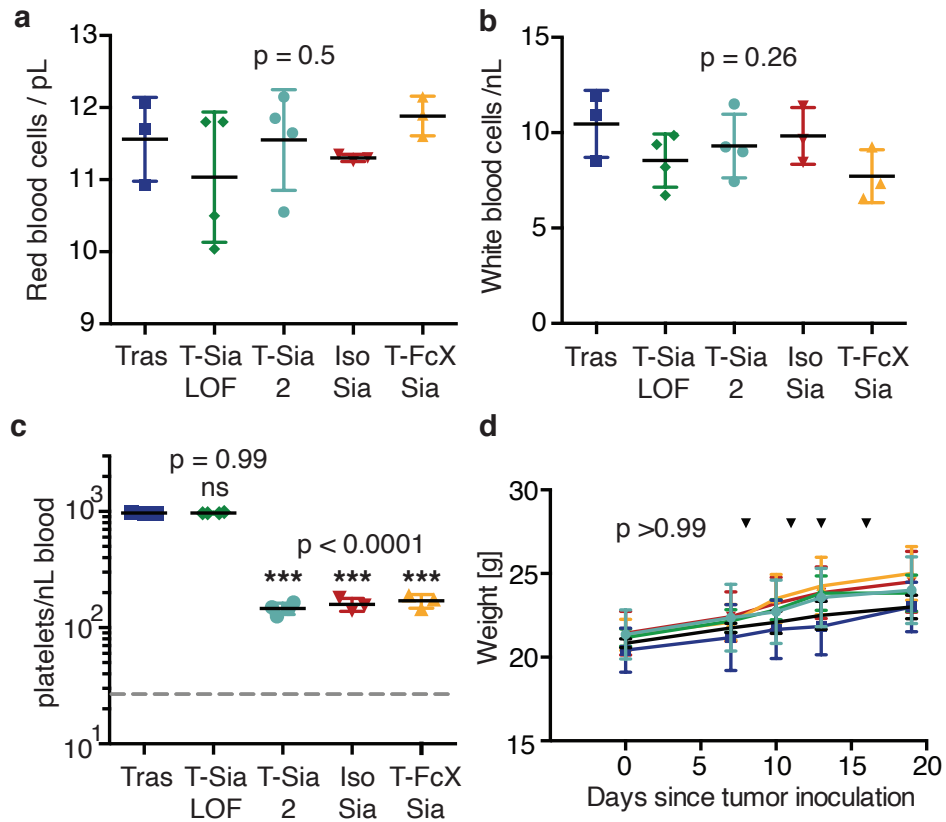
Supplementary Fig. 15. Development and characterization of Isotype-Sia, a nontargeting sialidase control. **a**, ESI-TOF mass spectrum of motavizumab expressed from Expi293 cells. **b**, ESI-TOF mass spectra of motavizumab light and heavy chains after partial heavy chain fGly conversion with tbFGE. **c**, ESI-TOF mass spectra of Isotype-HIPS-azide light chain (unchanged), and heavy chains (partially HIPS modified). **d**, ESI-TOF mass spectra of Isotype-Sia molecule. **e**, SDS-page gel of Isotype-Sia conjugate. **f**, Representative (n=3 independently run experiments) RP-HPLC trace of Isotype-Sia conjugate, absorbance detected at 280 nm, EAR = 1.2. **g**, Representative binding of Isotype-Sia to mouse Fc receptors as measured by BLI from n=2 independent experiments. Association was monitored for 20 s followed by dissociation for 40 s. Isotype-Sia binds all mouse Fcs except for Fc γ RIII, similar to trastuzumab.



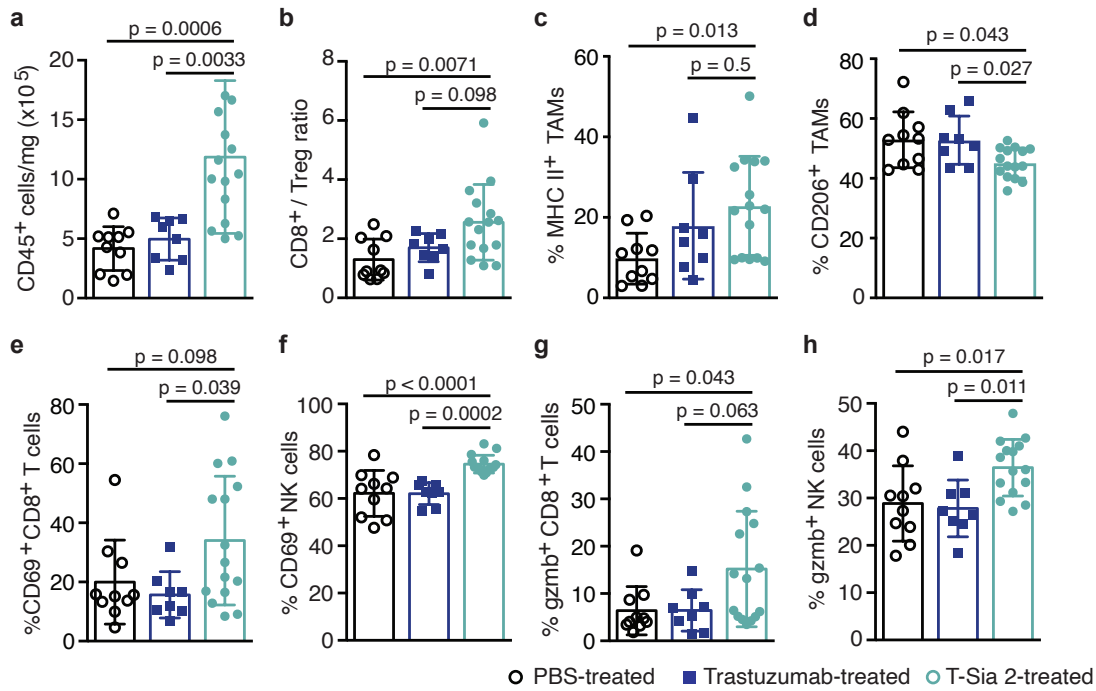
Supplementary Fig. 16. Development and characterization of T-FcX-Sia, a control with reduced effector recruitment. **a**, ESI-TOF mass spectrum of T-FcX expressed from Expi293 cells. **b**, ESI-TOF mass spectra of T-FcX light and heavy chain after aldehyde conversion with tbFGE. **c**, ESI-TOF mass spectra of T-FcX-azide light and heavy chains. **d**, ESI-TOF mass spectra of T-FcX-Sia molecule. **e**, SDS-page gel of T-FcX-Sia conjugate. **f**, Representative (n=3 experimental replicates) RP-HPLC spectrum of T-FcX-Sia, absorbance detected at 280 nm, EAR = 1.1. **g**, Representative binding of FcX-Sia to mouse Fc receptors as measured by BLI from n=2 independent experiments. Association was monitored for 20 s followed by dissociation for 40 s. The mutations made in the Fc domain of trastuzumab to make FcX eliminate binding to effector Fc receptors, but retain binding to the FcRn receptor critical for antibody half-life.



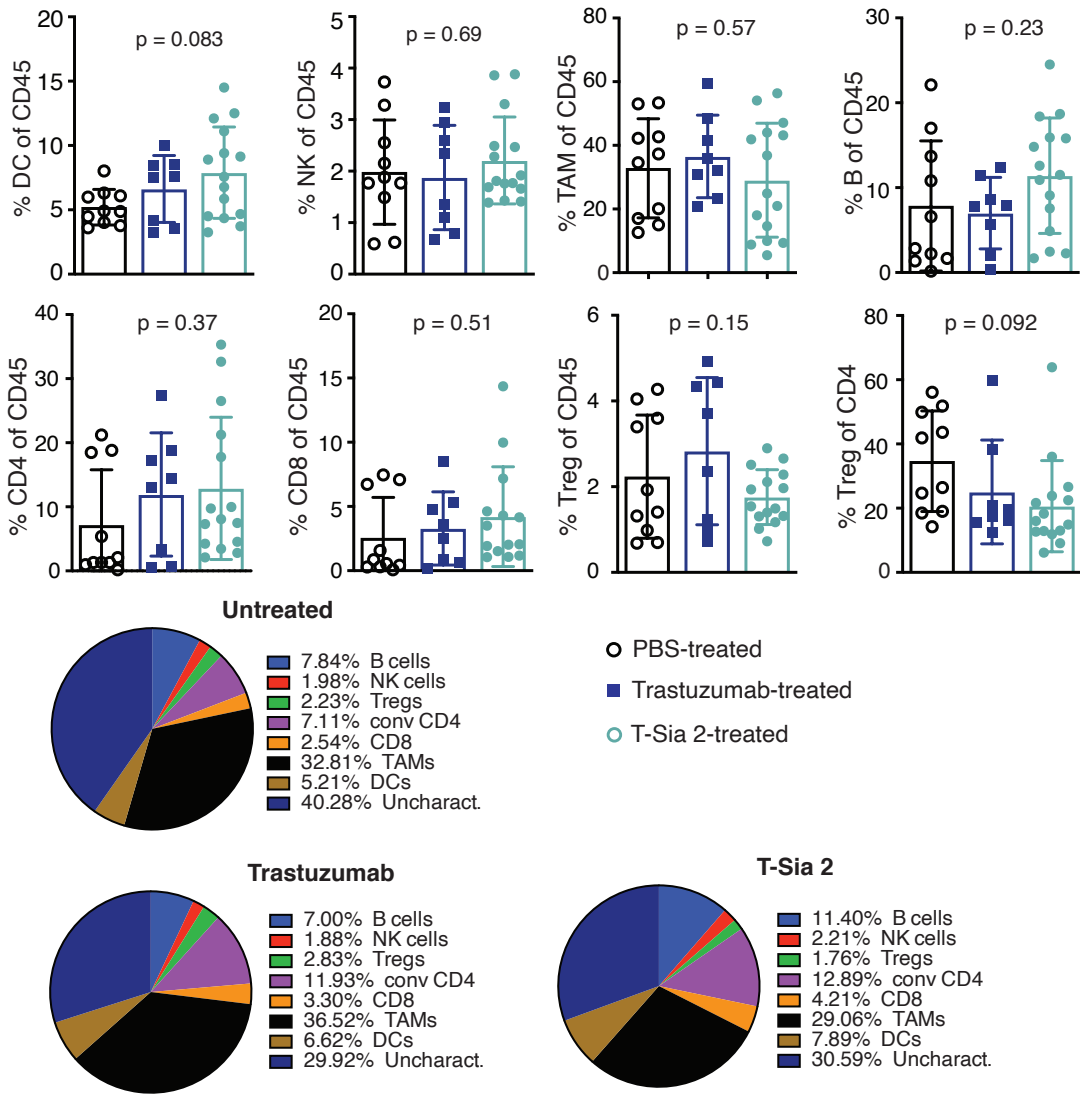
Supplementary Fig. 17. NK cell-mediated ADCC with control constructs. NK cell-mediated ADCC performed as in Fig. 5b on two additional control cell lines. (Left): MDA-MB-468 HER2⁻ control cell lines do not show any trends towards increased killing with increased antibody-sialidase construct concentration. (Right): SK-BR-3, the HER2-high expressing cell line demonstrates marked increase in ADCC with T-Sia 2, T-Sia LOF, and trastuzumab-treated cells, T-FcX is significantly reduced, and Isotype-Sia does not bind and desialylate target cells at these concentrations (all data points from n=3 experimental replicates are shown; a one-site - specific binding least squares fit was modeled onto the data with GraphPad Prism 6).



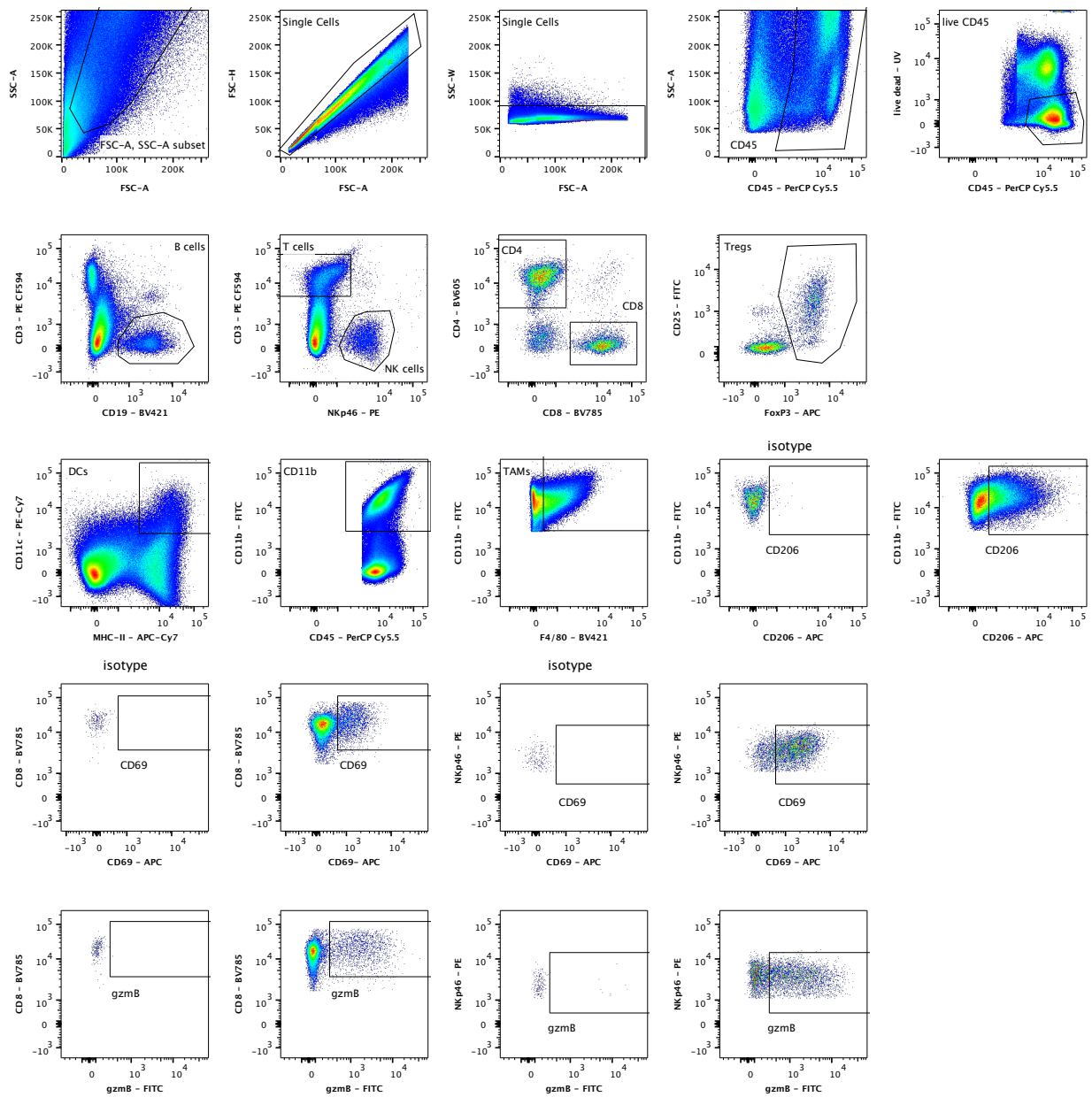
Supplementary Fig. 18. Blood cell counts and mouse weights following T-Sia 2 treatment. **a**, Red and **b**, white blood cell counts from mice depicted in Fig. 5c taken 2 days after first injection of conjugate therapy; ordinary one-way ANOVA (Mean counts \pm SD, n=3: PBS, Isotype-Sia, T-FcX-Sia, n=4: T-Sia-LOF, T-Sia 2). **c**, Platelet counts for the mice (depicted in Fig. 5c) 2 days after first injection of conjugate therapy; ordinary one-way ANOVA with Dunnett's multiple comparison test compared to trastuzumab-treated mice, (mean \pm SD, n=3: PBS, Isotype-Sia, T-FcX-Sia, n=4: T-Sia-LOF, T-Sia 2). **d**, Mouse weight measured 5x during treatment and tumor growth; ordinary two-way ANOVA revealed no significance in mouse weights over time compared to PBS control mouse (Mean \pm SD, PBS (n=6), trastuzumab (tras) (n=6), T-Sia-LOF (n=6), Isotype-Sia (n=6), T-FcX-Sia (n=7), or T-Sia 2 (n=7)).



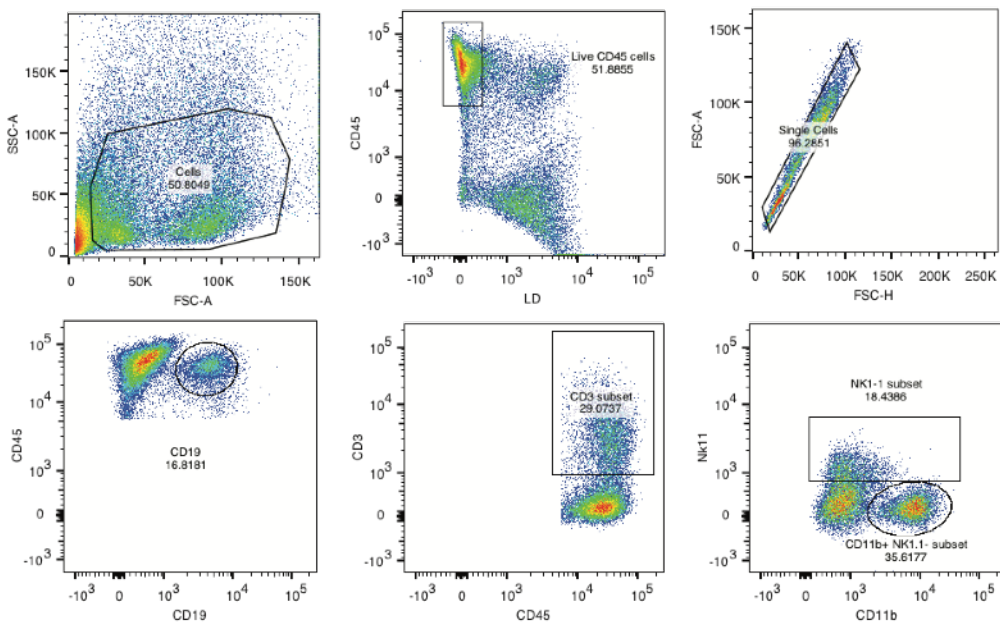
Supplementary Fig. 19. Analysis of TILs in the PBS-, trastuzumab-, and T-Sia 2-treated tumor microenvironment after sacrifice revealed enhanced activated immune infiltration. Analysis of tumor infiltrating leukocytes quantified from two independent mouse experiments (Figs. 4 and 5) of HER2⁺ EMT6 tumor-bearing mice treated with PBS (n=10), trastuzumab (n=8), and T-Sia 2 (n=15) revealed an increase in **a**, CD45⁺ cells per mg of tumor weight, as well as **b**, a larger CD8⁺ T cell to regulatory T cell ratio. Additionally, there was an apparent increase in **c**, MHC II⁺ TAMs and decrease in **d**, %CD206⁺ tumor-associated macrophages (TAMs). To investigate lymphocyte activation, %CD69⁺ was assessed in **e**, CD8⁺ T cells and **f**, NK cells, and %granzyme B⁺ was measured for **g**, CD8⁺ T cells and **h**, NK cells. The receptor expression levels were analyzed by an ordinary one-way ANOVA followed by a post hoc test (Dunnet's). Multiplicity-adjusted p-values are reported comparing PBS- and trastuzumab-treated tumors with T-Sia 2- treated mice (mean ± SD). CD8⁺ = CD8⁺ T cells.



Supplementary Fig. 20 Further analysis of tumor infiltrating leukocytes in PBS, Trastuzumab, and T-Sia 2. Above: analysis of tumor infiltrating leukocytes quantified from two independent mouse experiments (Figs. 4 and 5) of HER2⁺ EMT6 tumor-bearing mice treated with PBS (n=10), trastuzumab (n=8), and T-Sia 2 (n=15*). None of these results were statistically significant by one-way ANOVA (mean \pm SD displayed above). DC = dendritic cells, TAM = tumor associated macrophage, B = B cell, CD4 = CD4⁺ T cells, CD8 = CD8⁺ T cells. *n=14 for T-Sia 2-treated mice analyzed for the percent of CD45⁺ cells that are CD8⁺. Below: pie charts of percentages of TILs from PBS-, trastuzumab-, and T-Sia 2-treated mice.



Supplementary Fig. 21. Gating strategy for flow cytometry analysis of TILs.
Gating strategy for the results depicted in Supplementary Fig. 19 and 20.



Supplementary Fig. 22. Representative flow cytometry gating on tumor infiltrating leukocytes. Cells are gated first on FSC-A/SSC-A to remove debris, then live leukocytes are gated as CD45⁺ and Live/Dead (LD) stain negative. Single cells are gated using FSC-A/FSC-H, then those single cell gated CD45⁺ leukocytes are separated into CD19⁺ B cells, CD3⁺ T cells, NK1.1⁺ NK cells, and CD11b⁺ myeloid cells. Gating is representative of n=10 wt mouse tumors and n=12 Siglec-E^{-/-} from two independent experiments, thawed and analyzed on the same day.

Supplementary Note 1: Protein and DNA sequences

Protein Sequences

Protein	Amino Acid sequence
Trastuzumab light chain (and T-FcX light chain)	DIQMTQSPSSLSASVGDRVTITCRASQDVNTAVAWYQQKPGKAPKLLIYSASFVLYSGVPSRFS GSRSQTDFTLTISLQPEDFATYYCQQHYTPPTFGQGTVKEIKRTVAAPSVFIFPPSDEQLKS GTASVVCLNNFYPREAKVQWKVDNALQSGNSQESVTEQDSKDSTYLSSTTLSKADYEKH KYYACEVTHQGLSSPVTKSFNRGEC
Trastuzumab heavy chain	EVQLVESGGGLVQPGGSLRLSCAASGFNIKDTYIHWRQAPGKGLEWVARIYPTNGYTRYAD SVKGRFTISADTSKNTAYLQMNSLRAEDTAVYYCSRWGGDGFYAMDYWGGTLETVSSAST KGPSVFPLAPSSKSTSGGTAALGCLVKDYFPEPVTVSWNSGALTSGVHTFPAVLQSSGLYSL SSVTVPSSSLGTQTYICNVNHPKSNKVDKKVEPKSCDKHTCPCCPAPELLGGPSVFLFPPK PKDTLMISRTPEVTCVVVDVSHEDPEVKFNWYVGVEVHNAKTKPREEQYNSTYRVVSVLTVL HQDWLNGKEYKCKVSNKALPAPIEKTISKAKGQPREPVYTLPPSRDELTKNQVSLTCLVKGF YPSDIAVEWESNGQPENNYKTPPVLDSDGSFFLYSKLTVDKSRWQQGNVFSCVMHEALHN HYTQKSLSLSPGSLCTPSRGS
T-Fc-X heavy chain	EVQLVESGGGLVQPGGSLRLSCAASGFNIKDTYIHWRQAPGKGLEWVARIYPTNGYTRYAD SVKGRFTISADTSKNTAYLQMNSLRAEDTAVYYCSRWGGDGFYAMDYWGGTLETVSSAST KGPSVFPLAPSSKSTSGGTAALGCLVKDYFPEPVTVSWNSGALTSGVHTFPAVLQSSGLYSL SSVTVPSSSLGTQTYICNVNHPKSNKVDKKVEPKSCDKHTCPCCPAAPPVAGPSVFLFPPK PKDTLMISRTPEVTCVVVDVSHEDPEVKFNWYVGVEVHNAKTKPREEQYNSTYRVVSVLTVLHQ DWLNGKEYKCKVSNKALPAPIEKTISKAKGQPREPVYTLPPSRDELTKNQVSLTCLVKGFY PSDIAVEWESNGQPENNYKTPPVLDSDGSFFLYSKLTVDKSRWQQGNVFSCVMHEALHNH YTQKSLSLSPGSLCTPSRGS
Motavizumab light chain	DIQMTQSPSTLSASVGDRVTITCSASSRVGYMHWYQQKPGKAPKLLIYDTSKLASGVPSRFSG SGSGTEFTLTISSLQPDFATYYCFQGSGYPFTFGGGTKVEIKRTVAAPSVFIFPPSDEQLKSG TASVVCLNNFYPREAKVQWKVDNALQSGNSQESVTEQDSKDSTYLSSTTLSKADYEKH VYACEVTHQGLSSPVTKSFNRGEC
Motavizumab heavy chain	QVTLRESGPALVKPTQTLTCTSGFSLSTAGMSVGWIRQPPGKALEWLADIWWDDKKHYN PSLKDRRLTISKDTSKNQVVLKVTNMDPADTATYYCARDMIFNFYFDVWGQGTTVSSASTKG PSVFPLAPSSKSTSGGTAALGCLVKDYFPEPVTVSWNSGALTSGVHTFPAVLQSSGLYSLSSV VTVPSSSLGTQTYICNVNHPKSNKVDKKVEPKSCDKHTCPCCPAPELLGGPSVFLFPPKPK DTLTMISRTPEVTCVVVDVSHEDPEVKFNWYVGVEVHNAKTKPREEQYNSTYRVVSVLTVLHQ DWLNGKEYKCKVSNKALPAPIEKTISKAKGQPREPVYTLPPSRDELTKNQVSLTCLVKGFY PSDIAVEWESNGQPENNYKTPPVLDSDGSFFLYSKLTVDKSRWQQGNVFSCVMHEALHNHYT QKSLSLSPGSLCTPSRGS
ST Sialidase (N-HIS C-Ald)	MHHHHHHHGKIPNPLLGLDSTENLYFQGTVEKSVVFKAEGEHEFTDQKGNTIVGSGSGGTTKYF RIPAMCTTSKGTVVFADARHNTASDQSFIDTAARSTDGGKTWNKKIAIYNDRVNSKLSRVMD PTCIVANIQGRETILVMVGKWNNDKTWGAIRDKAPDTDWDLVLYKSTDGGVTFSKVETNIHD IVTKNGTISAMLGGVGSGQLNDGKLVFPVQMVRTKNITTVLNTSFIYSTDGITWSLPSGYCEGF GSENNIIEFNASLNVNNIRNSGLRRSFETKDFGKTWTTEFPPMDKKVVDNRNHGVQGSTITPSGNK LVAAHSSAQNKNNNDYTRSDISLYAHNLYSGEVKLIDAFYPKVGNAKGAGYSCLSYRKNDKET LYVVEANGSIEFQDLSRHLPIVIKSYNSLCTPSRGS
ST Sialidase Y369A (N-HIS C-Ald)	MHHHHHHHGKIPNPLLGLDSTENLYFQGTVEKSVVFKAEGEHEFTDQKGNTIVGSGSGGTTKYF RIPAMCTTSKGTVVFADARHNTASDQSFIDTAARSTDGGKTWNKKIAIYNDRVNSKLSRVMD PTCIVANIQGRETILVMVGKWNNDKTWGAIRDKAPDTDWDLVLYKSTDGGVTFSKVETNIHD IVTKNGTISAMLGGVGSGQLNDGKLVFPVQMVRTKNITTVLNTSFIYSTDGITWSLPSGYCEGF GSENNIIEFNASLNVNNIRNSGLRRSFETKDFGKTWTTEFPPMDKKVVDNRNHGVQGSTITPSGNK LVAAHSSAQNKNNNDYTRSDISLYAHNLYSGEVKLIDAFYPKVGNAKGAGYSCLSYRKNDKET LYVVEANGSIEFQDLSRHLPIVIKSYNSLCTPSRGS
ST Sialidase (original construct, no aldehyde Fig. 2a and Supplementary)	MHHHHHHHGKIPNPLLGLDSTENLYFQGTVEKSVVFKAEGEHEFTDQKGNTIVGSGSGGTTKYF RIPAMCTTSKGTVVFADARHNTASDQSFIDTAARSTDGGKTWNKKIAIYNDRVNSKLSRVMD PTCIVANIQGRETILVMVGKWNNDKTWGAIRDKAPDTDWDLVLYKSTDGGVTFSKVETNIHD IVTKNGTISAMLGGVGSGQLNDGKLVFPVQMVRTKNITTVLNTSFIYSTDGITWSLPSGYCEGF GSENNIIEFNASLNVNNIRNSGLRRSFETKDFGKTWTTEFPPMDKKVVDNRNHGVQGSTITPSGNK LVAAHSSAQNKNNNDYTRSDISLYAHNLYSGEVKLIDAFYPKVGNAKGAGYSCLSYRKNDKET LYVVEANGSIEFQDLSRHLPIVIKSYNSLCTPSRGS

Fig. 3,14a)	
VC sialidase	MRFKNVKKTALMLAMFGMATSSNAALFDYNATGDTEFDSPAQQGWMQDNTNNSGVLTNADGMPAWLVQGIGGRAQWTVSLSTNQAQASSFGWRMTTEMKVLGGMITNYANGTQRVLPIISLDSSGNLVVEFEGQTGRTVLATGTAATEYHKFELVFLPGSNPASFYFDGKLIRDNIQPTASKQNMIVWGNGSSNTDGAAYRDIKFIEQGDVIFRGPDRIPIVASVTPGVVTAFAEKRVGGDPGALSNTNDIITRTSRDGGITWDTELNLTEQINVSDFFDSDFDPRPIYDPSSNTVLSYARWPTDAAQNGDRIKPWMPNGIFYSVYDVASGNWQAPIDVTDQVKERSFQIAWGCGSELYRRNTSLSQQDWQSNAKIRIVDGAANQIQVADGSRKYVVTLSIDESGLVANLNGVSAPIILQSEHAKVHSFHDYELQYSALNHTTLFVDGQQITTWAGEVSQENNIQFGNADAQIDGRLHVQKIVLTQQGHNVEFDAFYLAQQTPEVEKDLEKLGWTIKTGNTMSLYGNASVNPGPCHGILTTRQQNISGSQNGRLIYPAIVLDRFFLNMSIYSDDGGSNWQTGSTLPFRWKSSSILETLEPSEADMVELQNGDLLTARLDFNQIVNGVNSPRQQFLSKDGGITWSLEANNANVFSNISTGTVDASITRFEQSDGSHFLFTNPQGNPAGTNGRQNGLWFSFDEGVTKGPIQLVNGASAYS DIYQLDSENAIVIVETDNSNMRILRMPITLLKQKLTLSQN
AU sialidase	MGHHHHHHHHHSSGHIEGRHMLEAPTPPNSPTLPPGSFSETNLAADRTAANFFYRIPALTYL GNDVVLAAWDGRPGSAADAPNPNISVQRRSTDGGKTWGPVQVIAGHVADASGPRYGYSDPSIYDAEANKVFAFFVYSKDQGFCCSFGNDDADRNVISSAVISSERTAGVTWSQPRLITSVTPKGTSKTNPAAGDVRNSNFASSGEIGIQLKYGPHKGRLIQQQYAGDVRQADGSNKIQAYSVYDDHGVTHKGANVGDRMDENKTELSDGRVLLNSRDNDANRGYRKVAVSTDGGATYGPVQSQDTELPDPANNGAIARMFPNAAQGSADAKKLIFTNANSKTGRENSARVSCDDGETWPGVRTIRSGFSAYSTVTRLADGKFGVLYEGNYTDNMPFATFDDAWLNYVCAPLAVPAVNIAPSATQEVPVTVNQEATTLSGATATVYTPSGWSATTVPVPDVAPGASVTVTVALTAPADASGPRSLNAAFTTADGRVSQFTFTATTPVAPQVGLTI
CP sialidase	MRGSHHHHHHTDPCNKNNTFEKNLDISHKPEPLILFNKDNNIWN SKYFRIPNIQLLNDGTILTFS DIRYNGPDDHAYIDIASARSTDGFKTWSYNIAMKNNRIDSTYSRVMMDSTTVITNTGRIILAGSWNTNGNWAMTTSTRSDWSVQMIYSDDNGLTWSNKIDLTKDSSKVKNQPSNTIGWLGGVGSGIVMDDGTIVMPAQISLRENNENNYYSLIYSKDNGETWTMGNKVPNSNTSENMIELDGALIMSTRYDYSGYRAAYISHDLGTTWEIYEPLNGKILTGKGSGCQGSFIKATTSNGHRIGLISAPKNTKGEYIRDNIAVYMIDFDDLSKGVQEICIPPEDGNKLGGSYSCLSFKNNHLGIVYEANGNIEYQDLTPYYI
MBP-tbFGE	MKSSHHHHHGSSMKIEEGKLVIWINGDKGYNGLAEVGKKFEKDTGIKVTVEHPDKLEEKFPQVAATGDGPDIIFWAHDRFGGYAQSGLLAEITPDFKAQDKLYPFTDAVRYNGKLIAYPIAVEALSLIYNKDLLPNPPKTWEIIPALDKELAKGKSA MFNLQEPYFTWPLIAADGGYAFKYENGKYDIKDVGVNAGAKAGLTFVLVDLIKHNMA DTYSIAEA AFNKG ETAMTINGPWAWSNIDTSKVNYGVTLPFKGQPSKPFVGVL SAGINAASP NKE LAKE FLEN YLLTDEGLEAVN KDKPLGAVALKSYEEELAKDPRIAATMENAQKGEIMP NIPQMSAFWYAVRTAVINAASGRQTVDEALKDAQTNSSSNNNNNNNNNLGIEENLYFQSNAMEVLT EVDLPGGSFRMGSTRFYPEEAPIHTVTVRAFVERHPVTNAQFAEFVSA TGYTVAEQPLD PGLY PGVDAADLC PGAM VFCPTAGPV DLR DW RQWWWDWVPGACWRHPFGRDS DIADRAGH PVVQVAYPD AVAYARWAGRRLPTEAEWEYAARG GTTATYAWGDQEKGPGMLMANTWQGRFPYRNDGALGWVGTSPVGRFPANGFGLDMIGNVWEWTTTEFYPHHRIDPPSTACCAPVKLATAADPTISQ TLKGGSHLCAPEYCHRYRPAARSPQSQDTATTHIGFRCVADPVG
GST-thrombin-Neu2	MSPILGYWKIKGLVQPTRLLLEYLEEKYEEHYERDEGDKWRNKKFELGLEFPNLPYYIDGDVKLTQSMAIIRYIADKHNM LGGCPKERA EISMLEGAVLDIRYGV SRI ASKDFETLKVDFLSKLPEMLKMFEDRLCKTYLNGDHVTHPDFMLYDALDVVLYMDPMCLDAFPKLVCFKKRIE AIPQIDKYLKSSKYIAWPLQGWQATFGGGDHPPKSDLVPRGSMASLPVQKESVFQSGAHAYRIPALLYLPQQQSLLAFAEQRASKKDEHAELIVLRRGDYDAPTHQVQWQQAQEVVAQARLDGHRSMNPCPLYDAQTGTLFLFIAIPGQVTEQQQLQTRANVTRLCQVTSTDHGR TWSSPRDLTDAAIGPAYREWSTFAVGP GHCLQLNDRARS LV PAYA YRKLHPIQRP IPSAFCFLSHDHGR TWARGHFVAQDTLECCQVAEVETGEQ RVV TLNARSHLRARVQA QSTNDLDFQESQLVKKLVEPPPQGCQGSVISFPSPRSGPGSPA QWLLYTHPTHSWQ RDLGAYLNP RPPA PEA WSEP VLLA KGSCA YSDLQSMGTGP DGSPLFGCL YEANDYEEIVFLMFTLKQAFPAEYLPLQLERPHRD
GST-thrombin-Neu3	MSPILGYWKIKGLVQPTRLLLEYLEEKYEEHYERDEGDKWRNKKFELGLEFPNLPYYIDGDVKLTQSMAIIRYIADKHNM LGGCPKERA EISMLEGAVLDIRYGV SRI ASKDFETLKVDFLSKLPEMLKMFEDRLCKTYLNGDHVTHPDFMLYDALDVVLYMDPMCLDAFPKLVCFKKRIE AIPQIDKYLKSSKYIAWPLQGWQATFGGGDHPPKSDLVPRGSEEVTTCSFNSPLFRQEDDRGITYRIPALLYIPPTHTFLAFAEK RSTR DEDALHLV LRRGLRIGQLVQWGPLKPLMEATLPGHRTMNPCPVWEQKSGCVFLFFICVRGHVTERQQIVSGRNAARLCFIY SQDAGCSWSEVRDLTEEVIGSELKHWATFAVGP GHGIQLQSGR LVIPAYTYYIPS WFFCFQLPCKTRPHSLMIYSDDLGVTWHGRLIRPMVTECEVAEV TGRAGH PVLYCSARTPNRCRAE ALSTDHGE GFQRL ALSRQLCEPPHGCQGSVIVSFRPLEIPHRCQDSSSKDAPTIQQSSPGSSLRLEEEAGTPSESWLLYSHPTS RQVRD LGIY

	NQTPLEAACWSRPWILHCGPCGYSDLAALEEEGLFGCLFECGTKQECEQIAFRLFTHREILSHL QGDCTSPGRNPSQFKSNLERPHRD
--	--

DNA sequences

Name	Sequence
<u>Sequence 1</u> Trastuzumab light chain DNA sequence including signal peptide (also the T-FcX light chain sequence)	ATGAGGGTCCCCGCTCAGCTCCTGGGGCTCTGCTGCTCTGGCTCCCAGGTGCAC GATGTGACATCCAGATGACCCAGTCCCCCTCCCTCCCTGCTGCCTCCGTGGCGAC AGAGTGACCATCACCTGTCGGGCCCTCCAGGATGTGAACACCGCCGTGGCTGGT ATCAGCAGAAGCCTGGCAAGGCCCCTAAGCTGCTGATCTACTCCGCTCCTCCTG TACTCCGGCGTGCCTCCGGTTCTCGGCTCCAGATCCGGCACCGACTTCACCC TGACCATCTCCAGCCTGAGGACTTCGCCACCTACTACTGCCAGCAGCAC TACACCACCCCTCCAACCTTCGGCCAGGGCACCAAGGTGGAGATCAAGCGTACGG TGGCTGCACCATCTGTCATCTTCCGCCATCTGATGAGCAGTTGAAATCTGGAA CTGCCTCTGTTGTGCCTGCTGAATAACTCTATCCCAGAGAGGGCAAAGTACAGT GGAAGGTGGATAACGCCCTCCAATCGGTAACTCCCAGGAGAGTGTACAGAGCA GGACAGCAAGGACAGCACCTACAGCCTCAGCAGCACCCGTGACGCTGAGCAAAGCA GAETACGAGAACACAAGTCTACGCCCTGCGAAGTCACCCATCAGGGCCTGAGCTC GCCGTACAAAGAGCTAACAGGGAGAGTGTGA
<u>Sequence 2</u> Trastuzumab heavy chain DNA sequence including signal peptide and C-terminal aldehyde tag NheI cut site in red BsrGI cut site in blue Used for generating T-FcX antibody	ATGGGTTGGAGCCTCATCTTGCTCTCCTTGCTGCTGTTGCTACGGGTGTCAC CGAAGTGCAGCTGGTGGAGTCTGGCGGAGGACTGGTGCAGCCAGGGGGCAGCCT GAGACTGTCTTGCAGCCTCCGGCTCAACATCAAGGACACCTACATCCACTGGG TCCGCCAGGCACCAGGCAAGGGACTGGAATGGGTGGGCCGGACTACCCCTACCAA CGGCTACACCAAGATAACGCCGACTCCGTGAAGGGCCGGTACCATCTCCGGCAGC ACCTCCAAGAACACCGCCTACCTGAGATGAATTCCCTGAGGGCCGAGGACACCG CCGTGTACTACTGCTCCAGATGGGAGGCGACGGCTTACGCCATGGACTACTG GGGCCAGGGCACCCCTGGTCACAGTGTCTCT GCTAGC ACCAAGGGCCCATGGTC TTCCCCCTGGCACCCCTCCAAGAGACACCTCTGGGGCACAGCGGCCCTGGGCT GCCTGGTCAAGGACTACTTCCCCGAACCGGGTGACGGTGTGTTGAACTCAGGCGC CCTGACCGGGCGTGACACCTTCCGGCTGTCTACAGTCCTCAGGACTCTACT CCCTCAGCAGCGTGGTGACCGTGCCTCCAGCAGCTGGGACCCAGACCTACAT CTGCAACGTGAATCACAAGCCCAGCAACACCAAGGTGGACAAGAAAGTTGAGGCCA AATCTTGTGACAAAACCTCACACATGCCACCGTGCCCAGCACCTGAACCTCTGGGG GGACCGTAGTCTCCTCTCCCCAAAACCCAAGGACACCCCTCATGATCTCCCG GACCCCTGAGGTACATGCGTGGTGAGCTGAGGACACGAAGACCCCTGAGGTC AAGTTCAACTGGTACGTGGACGGCGTGGAGGTGCTATAATGCCAAGACAAAGCCGC GGGAGGAGCAGTACAACAGCACGTACCGTGTGGTGACGGTCTCACCCTCTGCA CCAGGACTGGTGAATGCAAGGAGTACAAGTGAAGGTCTCCAACAAAGCCCTC CCAGCCCCATCGAGAAAACCATCTCCAAGGCCAAAGGGCAGCCCGAGAACACC AGG TGTAC CCCTGCCCTCATCCGGATGAGCTGACCAAGAACAGGTCTGAC GACCTGCCCTGGTCAAGGCTTCTATCCCAGCGACATGCCGTGGAGTGGAGAGC AATGGGAGCCGGAGAACAACTACAAGACCAAGCCCTCCGTGCTGGACTCCGACG GCTCCTCTTCTCTACAGCAAGCTACCGTGGACAAGAGCAGGTGGCAGCAGGG GAACGTCTTCTCATGCTCCGTGATGCATGAGGCTCTGCACAACCAACTACACCGAGA AGACCCCTCCCTGTCTCCGGTTCTCTGCACCCCTCCCGAGGTTCATGA
<u>Sequence 3</u> gBlock used to replace the amino acids "ELLG" with "PVA-" in the trastuzumab heavy chain to make Trastuzumab-FcX antibody.	AGTGCCTCT GCTAGC ACCAAGGGCCATGGTCTTCCCCCTGGCACCCCTCTCCA AGAGCACCTGGGGCACAGCGGCCCTGGCTGCCCTGGTCAAGGACTACTCTCC CGAACCGGTGACGGTGTGAGACTCAGGCCCTGACCGAGGGCGTGCACAC CTTCCCGCTGTCCTACAGTCCTCAGGACTCTACTCCCTCAGCAGCGTGGTACCG TGCCCTCCAGCAGCTGGCACCCAGACCTACATCTGCAACGTGAATCACAGCCC AGCAACACCAAGGTGGACAAGAAAGTTGAGGCCAAATCTGTGACAACAAACTCACAC ATGCCCAACCGTCCCCAGCACCTGAACCTCTGGGGGACCGTCAGTCTCCTCTCC CCCCAAACCCAAGGACACCCCTATGATCTCCGGACCCCTGAGGTACATGCGTG GTGGTGGACGTGAGGCCAGAAGACCTGAGGTCAAGTTCAACTGGTACGTGGACG GCGTGGAGGTGCTATGCCAAGACAAGCCGGGGAGGAGCAGTACAACAGCAC GTACCGTGTGGTACGCGTCTCACCGTCTGCACCGAGACTGGCTGAATGCAAG GAGTACAAGTGCAGGTCTCAACAAAGCCCTCCAGCCCCCATCGAGAAAACCAT CTCAAAGCCAAGGGCAGCCCCGAGAACACAGGT TGTAC CCCTGCCCT
<u>Sequence 4</u> gBlock for	ACCGGTGTACATTCCCAGGTACAACCTGCAGCAGCCTGGGGCTGAGCTGGTGAAGC CTGGGGCCTCAGTGAAGATGTCCTGCAAGGCTTCTGGCTACACATTACAGTTAC

Motavizumab (Isotype) antibody heavy chain variable sequence	AATATGCACTGGTAAAACAGACACCTGGTCGGGCCTGAATGGATTGGAGCTAT TTATCCCGAAATGGTATACTTCTACAATCAGAAGTCAAAGGCAAGGCCACATT GAETGCAGACAAATCCTCCAGCACAGCCTACATGCAGCTCAGCAGCCTGACATCTG AGGACTCTGCGGTCTATTACTGTGCAAGATCAGACTTACCGCGGTGACTGGTAC TTCAATGTCTGGGCGCAGGGACCACGGTACCGTCTGCAGCGTCGACCAAGG GC
<u>Sequence 5</u> gBlock for Motavizumab light chain variable sequence	ACCGGTGTACATT CAGACATACAGATGACCCAATCACCTTCCACGCTCAGCGCGTC TGTGGCGACCGCGTCACGATTACTTGTTCAGCGTCCTCTGGGTGCGGTACATGC ACTGGTACCGACAAAGGCCGGTAAAGCACCGAAGGTTGCTGATTACGATA CCTCC AAACTCGCTCTGGTGTCCC ATCCC GCTCAGCGGTTCAAGGGAGTGGTACCGAGTT TACACTGACTATTAGCAGTTGCAGCCGATGATTGCAACATACTACTGTTTCA GGGGAGTGGATACCCATTACGTTGGCGGGGGTACAAAGGTGGAGATAAACCGT ACGGTGGCTGCA
MBP-TEV-tbFGE	ATGAATCTTCACCATCACCACATGGTTCTTCTATGAAAATCGAAGAAGGT AAACTGGTAATCTGGATTAACGGGATAAAGGCTATAACGGTCTCGCTGAAGTCGG TAAGAAATTGAGAAAGATAACCGGAATTAAAGTACCGGTGAGCATCCGGATAAAACT GGAAGAGAAATTCCCACAGGGTGGCAACTGGCGATGGCCTGACATTATCTTCT GGGACACGACCGCTTGGTGGCTACGGCTAACATGGGCTGTTGGCTGAAATCACC CCGGACAAAGCGTCCAGGACAAGCTGATTGCTTACCGATCGCTGGGATGCCGTACGTTA CAACGGCAAGCTGATTGCTTACCGATCGCTGGTGAAGCGTTATCGCTGATTATAA CAAAGATCTGCTGCGAACCCGCCAAAACCTGGGAAGAGATCCGGCGCTGGAT AAAGAACTGAAAGCAGGAAAGGTAAAGAGCGCGCTGATGTTCAACCTGCAAGAACCGTA CTTCACCTGGCCGCTGATTGCTGCTGACGGGGTTATGCGTTCAAGTATGAAAAG GCAAGTACGACATTAAAGACGTTGGCGTGGATAACGCTGGCGCAAAGCGGGTCT GACCTTCTGGTTGACCTGATTA AAAACAAACATGAATGCAGACACCGATTACTC CATCGCAGAAGCTGCC TTAATAAAAGCGAAACAGCGATGACCATCAACGGCCGT GGGCATGGTCCAACATCGACACCGCAAAGTGAATTATGGTGAACGGTACTGCCG ACCTCAAGGGTCAACCATCCAAACCGTTGCTGGCGTGTGAGCGCAGGTATTAA CGCCGCCAGTCGAACAAAGAGCTGGCAAAGAGTCTCTCGAAAACATCTGCTGA CTGATGAAGGCTGGAAAGCGGTATAAAGACAACCGCTGGTGCCGTAGCGCT GAAGTCTTACGAGGAAGAGTGGCAAAGATCCACGTATTGCCGCACTATGGAAA ACGCCAGAAAGGTGAAATCATGCGAACATCCCGCAGATGTCGCTTCTGGTAT GCCGTGCGTACTGCGGTATCAACGCCGCGCAGCGGTGCGTCAACTGTCGATGAAG CCCTGAAAGACGCGCAGACTAATTGAGCTCGAACAAACAACAACAATAACA ACAACCTCGGGATCGAGGAAAACCTGTACTTCAATCCAATgcaATGGTGTGACCG AGTTGGTTGACCTGCCCCGGATCGTTCCGCATGGGCTCGACGCGCCTTACCC CGAAGAAGCGCCGATTCATACCGTGACCGTGCGCGCCTTGCCTGAGCGACAC CCGGTGACCAACCGCAATTGCCAATTGCTCTCCCGACAGGCTATGTGACGGT TGCAGAACACCCCTTGACCCGGCTTACCCAGGAGTGGACGCAGCAGACCTG TGTCCCGGTGCGATGGTGTGGTACCTGGCGCTGCTGGCGCCATCCGTTGGCC GGGACAGCGATATGCCGACCGAGCCGGCACCCGGTGTACAGGTGGCTATCC GGACGCCGTGGCTACGCCACGATGGGCTGGCGACGCCATCCGACCGAGGCCGA GTGGGAGTACCGGGCCCGTGGCGGAACCACGGCAACCTATGCGTGGGGCGACCA GGAGAAGCCGGGGGATGCTCATGGCGAACACCTGGCAGGGCGGGTTCTTAC CGAACACGGTGCATTGGCTGGGAAACCTCCCCGGTGGCAGGTTCCG GCCAACGGGTTGGCTGCTGACATGATCGGAAACGTTGGAGTGGACCAACCA CCGAGTTCTATCCACACCATCGCATCGATCCACCTCGACGGCCTGCTGCGCACCG GTCAAGCTCGCTACAGCCCGACCCGACGATCAGCCAGACCTCAAGGGCGGCT CGCACCTGTGCGCGCCGGAGTACTGCCACCGCTACCGCCGGCGCGCTCGC CGCAGTCGAGGACACCGGACCCATATCGGGTCCGGTGCCTGGCCGACCC GGTGTCCGGTAG
AU Sialidase from AU54pETd*	ATGGGCCATCATCATCATCATCATCATCACAGCAGCGGCCATATCGAAGGT CGTCATATGCTGAGGGCCCCACTCCGCCAATTGCCACGCTCCACCGGGCA GCTTCTCTGAAACCAATCTGGCGGCCGACCGCACGGCGGAATTCTTCTACCGG ATTCCCGCGCTTACCTACCTGGCAACGACGCTGGCTTGCAGCGTGGACGGTC GCCCGGGTTGGCGGGACGCCGAACCCGAACCTCGATCGTCCAGCGCCGA GCACGGACGGTGGCAAGACCTGGGGCCGGTCAAGTGTATGCCCGCAGGCCACG TCGCCGATGCCAGCGGCCCTCGATACGGCTACAGCGATCCCTCGTACATCTACGA CGCGGAAGCCAACAAGGTCTCGCTTCTCGTACTCGAAGGACCAAGGTTTG GCCAGTCAGTTGGCAACGACGACGCCGGAACGTCATTCTCCCGCGT CATCGAGTCTTCGACGCCGGTGCACATGGAGCCAGCCCCGCCATCACCTCC

	GTCACCAAGCCGGGTACCAGCAAGACCAACCCGGCAGCCGGCACGTCGCTCCA ACTTGCCTCCGGTGAGGGCATCCAGCTCAAATACGGCCGCACAAGGGCG TCTCATCCAGCAGTACGCCGGCACGTGCGCAAGCTGACGGAAGCAACAAGATC CAGGCCTACAGCGTCTATTGAGACGATCACGGCGTACGTGGCACAGGGTGCCA ACGTGGCGACCGGATGGACGAGAACAGACTGTGGAACGTGTCGACGGTCGGG CCTGCTCAACTCCCGGGACAACGCCAACCGGGCTACCGCAAGGTGGCCGCTCC ACGGACGGCGAGGCCACGTACGGCCCCGTAGCCAGACCGAACATTGCCGGAC CCTGCCAACACGGTGAACTGCCCGCATGTTCCCAACGCCGGCAGGGCTCCG CAGACGCGAAGAACACTGATCTTACCAACGCCAACCTGGCGCGAAC GTCTCGGCCCCGGTCTCTGTGACGACGGCAAACCTGGCGGTCCGCACC ATCCGTTCCGGCTTCTCGGCCACTCAACAGTGACCCGCTGGGGACGGAAGTT CGCGTCCCTACGAGGGCAACTACACGGAACATGCCCTCGCACCTCGAC GACCGTGGTTGAACTACGTCTGCGCTCCCTGGCAGTACCGGAGTCACATCG CCCCGAGGCCAACCGAGGAGTCCGGTACCGTCAACACAGGAAGCAACAC GCTTCCGGCGCGACCGCACTGTCATACGCCGTGCGGTGACTGACCGTGA GTGCCGTGCCCAGCCTGCGCAGCCTCACCGTACCGTACCGTGA CCGACCGGGCGGACGCCAGTGGCCCGCAGCCTCACCGTACCGTACCGACGG CGGATGGCCGGGTTCCGAGTCACCTCACCGCCACCCACGCCGTGGCTCCGCA AGTGGCCTTACCATCTAA
CP sialidase pET22b-T5-A99	ATCGGTGGGTCGCATCACCACCAACACCGATCCTGTAATAAGAATAACAC ATTGAGAAAAACCTGGATATTCTCACAAACCGAACCTCTGATTCTGTTAATAAG GATAACAACATTGGAATTCAAATACTTCTGATTCAAACATTCAACTCCTGAATG ACGGTACGATTCTTACCTTCCGACATCCGGTATAATGGGCCGGATGATCACGCAT ATATTGATATCGCGAGCGCTCGCTTACCGACTTGGTAAACGTTGGAGCTATAACA TTGCGATGAAAACAACCGGATTGACAGTACATATTCACTGTCATGGATTCAACGA CCGTAATTACTAACACCGCCGTATTATTCTGATCGCAGGCTCGGGAAATACAAACG GTAATTGGGCAATGACGACTTCTACCCGTCGTTCTGACTGGAGCGTTAGATGATC TACAGTACGATAACGGACTGACGTGGTCAAATAAAATCGATCTGACGAAAGACTC AAGCAAAGTGAAGAACCGCCTCAAATACCATGGCTGGCTTGGGGTTGGT CGGTATTGTTATGGATGATGGCACCATTGTTATGCCCTGCGCAGATCAGTTACGC GAAAATAATGAGAACATTATTAGCCTGATTATTCAAAGGATAACGGCGAAA CGTGGACTATGGCAATAAAAGTGCAGACAGTAACACCTCAGAGAACATGGTATC GAGCTGGATGGTCTGATTATGTCACCCGTTACGATTACAGCGGTATCGCGC CGCTACATCTCGCATGATCTGGGACCACGTGGAGATTATGAAACCTCTGAACG GAAAATTTGACTGGTAAAGGTTAGGCTGCCAAGGCTCTTCAAAAGCGACCA CCAGCAACGGGCATCGTACGGACTGATTTCTGCCCTAAAAACACCAAAGGCAG TACATTGCGATAACATGCCGTGACATGATTGATTTGATGACCTCTCAAAAGGC GTGCAGGAGATTGATCCGATTCAGAAGATGGCAACAAACTGGTGGGGGTA CTCGTGTCTGTCATTTAAAAAACCACATGGGAAATTGTTGACGAAGCGAACGGAA TATTGAATATCAGGACCTGACCCCGTACTATATC
<u>GST-thrombin-</u> <u>Neu2</u>	ATGTCCTCTACTAGGTTATTGGAAAATTAGGGCTTGTGCAACCCACTCGACTT CTTTGGAATATCTTGAAGAAAAATATGAAGAGCATTGATGAGCGCGATGAAGGT GATAATGGCGAACAAAAAGTTGAATTGGGTTGGAGTTCCCAATCTCCTTATT ATATTGATGGTATGTTAAATTAAACACAGTCTATGCCCATACGTTATAGCTGA CAAGCACACATGTTGGGTTGTCAAAAGAGCGTGCAGAGATTCAATGCTTG AAGGAGCGGTTTGGATATTAGATACGGTGTTCGAGAATTGCAATAGTAAAGACT TTGAAACTCTCAAAGTTGATTTCTTAGCAAGCTACCTGAAATGCTGAAATGTCGA AGATCGTTATGTCATAAAACATATTAAATGGTATGATGTAACCCATCCTGACTTC ATGTTGATGACGCTCTGATGTTTTATACATGGACCAATGTGCCTGGATGCG TTCCTAAAATTAGTTGTTTTAAAAACGTATTGAAGCTATCCCACAAATTGATAAGT ACTGAAATCCAGCAAGTATAGCATGGCCTTGCAGGGCTGGCAAGCCACGTT GGTGGTGGCGACCATCCTCCAAAATCGGATCTGGTCCCGTGGATCCATGGCGT CCCTCCTGTCCTGCAAGAGGAGAGCGTGTCCAGTCGGAGCCATGCCACAG AATCCCTGCCCTGCTCACCTGCCCTGGCAGCAGTCCTGCTGCCCTCGCGAA CAGCGGGCAAGCAAGAAGGATGAGCACGCAGAGCTGATTGCTCGCGCAGAGGAG ACTACGACGCACCCACCCACCGAGGTTAGTGGCAAGCTCAGGAGGTGGGCCCA GGCCCGGCTGGATGGCCACCGGTTCCATGAACCCATGCCCTTGATGACGCGCAG ACGGGGACCCCTCTCCTCTTCAATTGCCATCCCTGGCAAGTCACGGAGCAACA GCAGCTGCAGACCAGGGCAATGTGACGCGCTGTGCCAAGTCACCGACTGAC CACGGGAGGACCTGGAGCTCCCCCAGAGAACCTCACTGATGCGGCCATGGCCCA CCTACCGGGAGTGGTCCACCTTGCAGTGGGCCGGGGATTGTTGAGCTTAA CGACAGGGCCGGAGCCTGGTGGGCCCTACGCCCTACCGGAAACTCACCCCC

	ATCAAAGGCCGATCCCTCTGCCTCTGCTCCTCAGCCATGACCATGGCGCAC GTGGCGCGAGGGCACTTGTGGCCCAGGACACCCCTGGAGTGCCAGGTGGCGA AGTCGAGACTGGGAGCAGAGGGTGGTGAACCTCAACCGAGAACGCCACCTCCGA GCCAGGGTCCAGGCCAGAGCACCAATGACGGGCTGATTCCAGGAGTCTCAGC TGGTAAGAAGCTGGTGAGCCGCCAGGGCTGCCAGGGAGCGTCATCA GCTCCCCCAGCCCCGCTCGGGGCTGGCTCCAGGCCAGTGGCTGCTACAC TCACCCACACACTCTGGCAGAGGGCCGACCTGGGTCCTACCTCAACCGCGA CCTCAGCCCCGAGGCTGGTCAAGAGCGGTACTGCTGGCAAGGGCAGCTGTG CCTACTCAGACCTCCAGAGCATGGCACCGGCCCTGATGGGCCCCCTGTTGG GTGCTGTACGAAAGCAAATTGACGAGGATTGTCTTCTATGTTCACCTGAA GCAAGCCTCCAGCTGAGTACCTGCCTCAGCTCGAGCGGCCGATCGTGAC
GST-thrombin- Neu3	ATGCCCCCTACTAGGTTATTGGAAAATTAGGGCCTGTGCAACCCACTCGACTT CTTTGGAATATCTGAAGAAAAATATGAAGAGCATTGTATGAGCGCGATGAAGGT GATAATGGCAAACAAAAAGTTGAATTGGGTTGGAGTTCCCAATCTCCTTATT ATATTGATGGTATGTTAAATTAAACACAGTCTATGGCATACGTTATATAGCTGA CAAGCACACATGTTGGGTGGTGCACAAAGAGCGTGCAGGAGATTCAATGCTT AAGGAGCGGTTGGATATTAGATACGGTGTTCAGAAGATTGCATATAGTAAAGACT TTGAAACTCTCAAAGTTGATTTCTTAGCAAGCTACCTGAAATGCTGAAAATGTCGA AGATCGTTATGTCATAAAACATATTAAATGGTATCATGTAACCCATCCTGACTTC ATGTTGATGACGCTCTTGTATGGTCTTACATGGACCCAATGTCCTGGATGCG TTCCAAAATTAGTTGTTAAAAAACGTATTGAAGCTATCCCACAAATTGATAAGT ACTGAAATCCAGCAAGTATATAGCATGGCCTTGCAGGGCTGGCAAGCCACGTT GGTGGTGGCGACCATCCTCAAAATCGGATCTGGTCCCGTGGATCCGAGGAGG TTACCCACCTGCAGCTTAACCCCCTTGTTGCCCCAACCCATACTTTTGGCATTG CATATCGCATTCCGCCCTTGTACATTCCCCAACCCATACTTTTGGCATTG TGAGAACGTTTACCCCGCGTGTGAGGATGCGTTACACTAGTGTGCGCCGTG GTCTCGCATCGGACAATTAGTACAGTGGGCTTTAAACCGCTTATGGAAGCG ACCTTACCAAGGACATCGTACTATGAACCCCTGCTGTGTTGGAAACAGAAATCTGG CTCGTGTCTTATTCTTATCTGCGTACGTGTCACGTAACAGAACGCCAGCAAAT TGTAAGTGGCCGTACCGGCCGCTTGTGTTATCTACTCGCAGGATGCGGGAT GTTCTGGTCAAGGGTCCGTGACCTGACAGAGGGAGGTTATGGGCTGAGTTAAA CACTGGGCCACTTCGCGTAGGTCAGGTCTGGATCCAGTTGCACTGGGAC GCCTGGTTATCCGGTTATACTTACTATATCCCGTGTGGTTCTTGTGTTCAACT GCCCTGTAAGACGCGTCCACACTCGCTGTGATCTATAGCGATGATTGGAGGTTA CGTGGCATCGGACGTTGATCCGGCGAGACATCCAGTGTGACTGTTCAAGCGTACGCC CGAAGTGAAGGGCGCAGGACATTTCAACGGATCATGGTAAGGCTTCAACGCC AATCGCTGCGTGCAGGAAAGCACTTCAACGGATCATGGTAAGGCTTCAACGCC TGCCTTATCAGCCAACGTGCGAACGCCATGGGTGTCAGGGCAGCGTGGTT CATTCCGCCACTGGAAATTCCCATGTTGCAAGACTCCTCTAGCAAAGATGCC CCTACGATCCAACAGTCGAGTCTGGTAGTAGCCTGCCCTGAGGAAGAACAG GAACGCCGTGAGTCTGGTTATTACAGGCCATCCAACGTCCTGTAAGCAGCGT GTGGACTTAGGTATCTACTAAACCAAACCCCCCTGAGGCCGCTGTTGGAGGCC TCCCTGGATTCTGCACTGTGGCCCTGCGGATATTCAAGATTGGCGCCCTTGAAG AGGAAGGGCTTGTGCGCTTTATTGAATGTGGCACAAAGCAAGAATGCGAACAA ATCGCCTCCGTTATTACTCATCGCGAGATTGAGGCCACTTACAGGGAGACTGT ACGTCGCCTGGACGTAATCCCTCCAATTCAAGTCTAACCTCGAGCGGCCGATCG TGACTGA

Supplementary Note 2: Synthetic Procedures

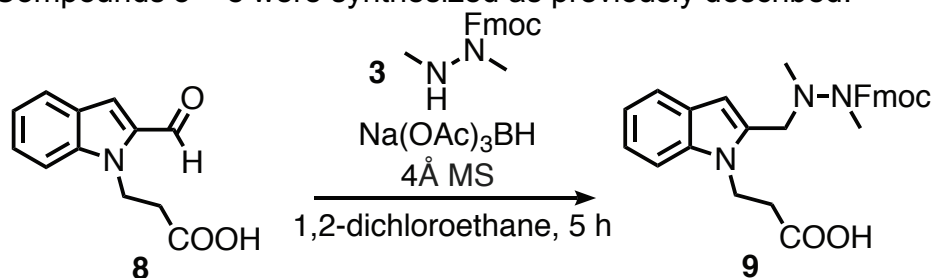
General synthetic chemistry instrumentation

Molecular sieves (Sigma-Aldrich, 688363) were flame-dried under vacuum and used immediately after cooling. Thin layer chromatography was conducted on SiliCycle silica plates (TLG R10011B-624) or C18 silica gel TLC plates (Analtech, 55077), with detection of multiband UV-absorption (254 – 365 nm). Column chromatography was done with Biotage SNAP KP-Sil (FSK0-1107) or Ultra C18 (FSUL-0401) flash purification cartridges (10 - 120 g) and an Isolera Prime ACI automated fraction collector from Biotage. The preparative RP-HPLC instrument used in this manuscript consists of an Agilent Technologies ProStar 325 UV-vis detector, two PrepStar solvent delivery modules, and a 440-LC fraction collector. The column for prep RP-HPLC was a Varian Microsorb 100 Å C18, 8 µm, 21.4 × 250 mm Dynamax preparative column (R0080220G8).

Proton nuclear magnetic resonance (^1H NMR) and proton-decoupled carbon-13 nuclear magnetic resonance (^{13}C { ^1H } NMR) spectra were obtained on Mercury-400 and Varian-400 NMR spectrometers at 25 °C, are reported in parts per million downfield from tetramethylsilane, and are referenced to the residual protium or carbon resonances of the NMR solvent (CDCl_3 : 7.26 (^1H), and 77.16 (^{13}C), [CHCl_3]). MestReNova v12.0.3 was used for all chemical NMR analysis. Data are represented as follows: chemical shift, multiplicity, coupling constants in Hertz (Hz), and integration. Splitting patterns are designated as follows: br = broad, s = singlet, d = doublet, t = triplet, q = quartet, quin = quintet, sept = septet, m = multiplet, dd = doublet of doublet, dt = doublet of triplet. NMR signals were assigned on the basis of ^1H , ^{13}C , COSY, and HSQC experiments. Low resolution mass spectra of small molecules were recorded using an Agilent 1260 Infinity Quaternary LC and 6120 Quadrupole LCMS System. High resolution mass spectra of small molecules and proteins were performed by the Stanford University Mass Spectrometry (SUMS) core facility and recorded on an Agilent 1260 HPLC, a Bruker MicroTOF-Q II ESI-Qq-TOF, and a Thermo Exactive benchtop Orbitrap mass spectrometer. Mass spectrometry of digested proteins was performed on Orbitrap Fusion Tribrid mass spectrometer (Thermo Fisher Scientific).

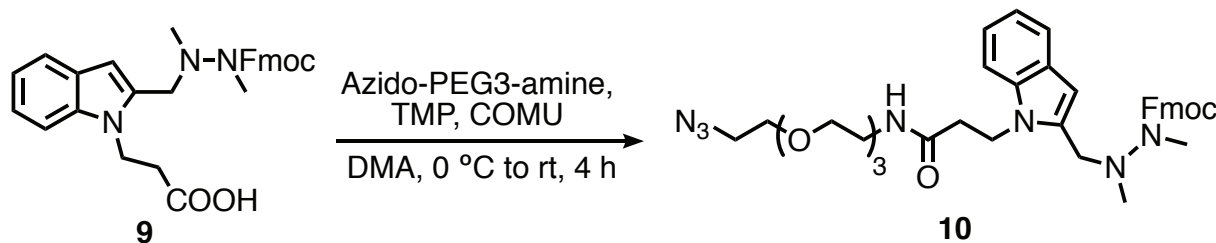
Synthesis of Azido-PEG3-HIPS

Compounds **3** – **8** were synthesized as previously described.^{27,28}

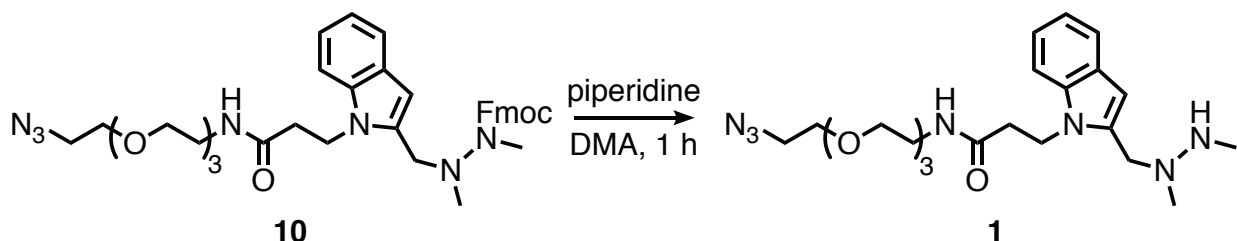


3-(2-((9H-Fluoren-9-yl)methoxy)carbonyl)-1,2-dimethylhydrazinylmethyl)-1H-indol-1-ylpropanoic acid (9): Prepared using a published procedure²⁸ with modified purification. To a solution of **8** (423 mg, 1.95 mmol, 1 equiv.) and (9H-fluoren-9yl)methyl 1,2-dimethylhydrazinecarboxylate, **3**, (1.08 g, 3.83 mmol, 2 equiv.) in 1,2-

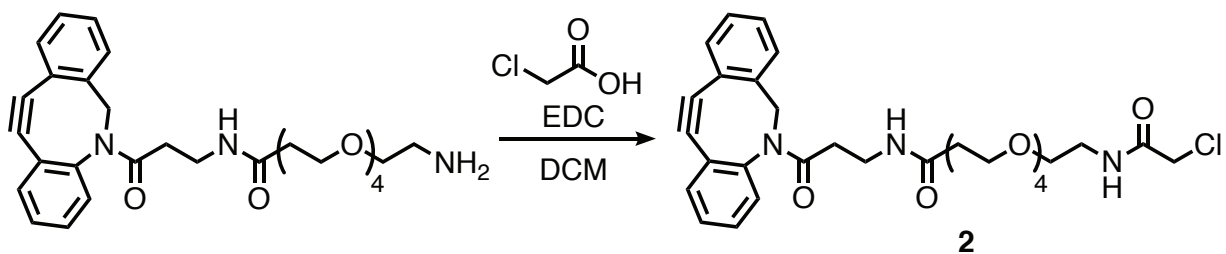
dichloroethane (53 mL) with 4Å MS was added sodium triacetoxyborohydride (519 mg, 2.45 mmol, 1.3 equiv.). The resulting yellow suspension was stirred for 5 h and then quenched with NaHCO₃ (saturated aqueous solution, 10 mL), followed by addition of HCl (1 M aqueous solution) to pH 4. The organic layer was separated, and the aqueous layer was extracted with CH₂Cl₂ (5 x 10 mL). The pooled organic extracts were dried over Mg₂SO₄, filtered, and concentrated to an orange oil. Purification by HPLC (20-90% ACN in water) gave **9** as an orange solid (821 mg, 1.70 mmol, 87%). The spectral data were in agreement with literature values²⁸.



(9H-Fluoren-9-yl)methyl 2-((1-(1-azido-13-oxo-3,6,9-trioxa-12-azapentadecan-15-yl)-1H-indol-2-yl)methyl)-1,2-dimethylhydrazinecarboxylate (10): A solution of **9** (1.2 g, 2.48 mmol, 1 equiv.) and 11-azido-3,6,9-trioxaundecan-1-amine (Azido-PEG3-amine) (819 µL, 3.72 mmol, 1.5 equiv.) in anhydrous dimethylacetamide (DMA) (9.92 mL) was cooled to 0 °C. Then, 2,4,6-trimethylpyridine (TMP) (655 µL, 4.96 mmol, 2 equiv.) and COMU (1.09 g, 2.48 mmol, 1 equiv.) were added and the reaction was stirred at 0 °C for 30 min, then warmed to RT and stirred for 4 h. The reaction mixture was diluted with ethyl acetate (150 mL), washed with 1 M HCl (3x 25 mL), 1 M NaHCO₃ (3x 25 mL), and brine (3x 25 mL), dried over MgSO₄, filtered, and concentrated to a viscous orange oil. Purification via C18 reversed-phase silica gel flash column chromatography (0-90% ACN in water) gave **10** as a light brown oil (1.26 g; 1.84 mmol; 75%). **TLC:** (water:ACN, 10:90 v/v) R_f = 0.72; (MeOH:DCM, 10:90 v/v) R_f = 0.52. **¹H NMR:** (400 MHz, CDCl₃) δ 7.69 (d, J = 7.6 Hz, 2H, 2x Ar-CH Fmoc), 7.54 – 7.39 (m, 3H, 2x Ar-CH Fmoc & Ar-CH indole), 7.38 – 7.28 (m, 3H, Ar-CH indole & 2x Ar-CH Fmoc), 7.27 – 7.15 (m, 2H, 2x Ar-CH Fmoc), 7.15 – 7.02 (m, 2H, Ar-CH indole & NHCO), 6.99 (t, J = 7.4 Hz, 1H, Ar-CH indole), 6.28 (s, 0.68H, Ar-CH indole), 5.95 (s, 0.44H), 5.82 (s, 0.38H), 4.65 – 4.21 (m, 4H, CH₂ Fmoc & CH₂-N indole), 4.15 (t, J = 6.1 Hz, 1H, CH Fmoc), 4.06 – 3.93 (m, 1H, CH₂-NMe), 3.55 – 3.41 (m, 6H, 3x CH₂ PEG), 3.39 (dd, J = 5.8, 3.5 Hz, 2H, CH₂ PEG), 3.34 – 3.14 (m, 8H, 2x CH₂ PEG & CH₂-NHCO & CH₂-N₃), 2.82 – 2.72 (m, 3H, N-Me), 2.68 – 2.35 (m, 5H, CH₂-CO & N-Me). **¹³C NMR:** (101 MHz, CDCl₃) δ 171.68 (NHCO), 155.50 (NCOO), 143.72 (2x Ar-C Fmoc), 141.17 (2x Ar-C Fmoc), 137.03 (Ar-C indole), 134.63 (Ar-C indole), 127.62 (2x Ar-CH Fmoc), 127.21 (Ar-C indole), 127.00 (2x Ar-CH Fmoc), 124.83 (2x Ar-CH Fmoc), 121.70 (Ar-CH indole), 120.39 (Ar-CH indole), 119.87 (2x Ar-CH Fmoc), 119.43 (Ar-CH indole), 109.52 (Ar-CH indole), 103.32 (Ar-CH indole), 70.34 (CH₂ PEG), 70.26 (CH₂ PEG), 70.17 (CH₂ PEG), 69.83 (CH₂ PEG), 69.71 (CH₂ PEG), 69.28 (CH₂ PEG), 67.15 (CH₂-N indole), 50.63 (CH₂-NMe), 50.41 (CH₂-N₃), 47.07 (CH Fmoc), 40.34 (CH₂-OCO), 39.82 (CH₃-N), 39.21 (CH₂-NHCO), 36.86 (CH₂CONH), 30.75 (CH₃-N). **ESI-HRMS:** calc'd for C₃₇H₄₅N₇NaO₆ [M+Na]⁺:706.3324; found: 706.3339.



N-(2-(2-(2-azidoethoxy)ethoxy)ethyl)-3-(2-((1,2-dimethylhydrazinyl)methyl)-1H-indol-1-yl)propanamide (1): **10** (95 mg, 138 µmol, 1 equiv.) was added to a stirred solution of piperidine (274 µL, 2.76 mmol, 20 equiv.) in DMA (1.38 mL) at RT. The reaction mixture was stirred for 1 h and directly purified via C18 reversed-phase silica gel flash column chromatography (0-100% ACN in water) affording azido-PEG3-HIPS (**1**) as light yellow solid (54.6 mg, 118 µmol, 86%) containing some impurities. This compound appeared to degrade in light and air and was therefore used at this purity and stored at -80 °C under argon. **TLC:** (water:ACN, 10:90 v/v) R_f = 0.72; (MeOH:DCM, 10:90 v/v) R_f = 0.52. **¹H NMR:** (400 MHz, CDCl₃) δ 7.47 (d, *J* = 7.5 Hz, 1H, Ar-CH), 7.30 (d, *J* = 8.4 Hz, 1H, Ar-CH), 7.11 (t, *J* = 7.6 Hz, 1H, Ar-CH), 7.00 (t, *J* = 7.4 Hz, 1H, Ar-CH), 6.31 (s, 1H, Ar-CH), 6.05 (s, 1H, NH), 4.54 (t, *J* = 7.5 Hz, 2H, CH₂-N indole), 3.80 (s, 2H, CH₂-NMe), 3.53 (m, 6H, 3x CH₂ PEG), 3.49 – 3.44 (m, 2H, CH₂ PEG), 3.39 – 3.34 (m, 2H, CH₂ PEG), 3.27 (d, *J* = 9.7 Hz, 6H, CH₂ PEG & CH₂-N₃ & CH₂-NHCO), 2.63 (t, *J* = 7.2 Hz, 2H, CH₂-CO), 2.53 (s, 3H, N-Me), 2.35 (s, 3H, N-Me). **¹³C NMR:** (101 MHz, CDCl₃) δ 170.82 (CONH), 137.19 (Ar-C), 135.92 (Ar-C), 127.68 (Ar-C), 121.70 (Ar-CH), 120.49 (Ar-CH), 119.66 (Ar-CH), 109.62 (Ar-CH), 103.17 (Ar-CH), 70.78 (CH₂ PEG), 70.66 (CH₂ PEG), 70.60 (CH₂ PEG), 70.25 (CH₂ PEG), 70.13 (CH₂ PEG), 69.74 (CH₂ PEG), 55.93 (CH₂-NMe), 50.75 (CH₂-N₃), 43.47 (CH₃-N), 40.21 (CH₂-N indole), 39.36 (CH₂-NHCO), 37.20 (CH₂-CO), 35.24 (CH₃-N). **ESI-HRMS:** calc'd for C₂₂H₃₆N₇O₄ [M+H]⁺: 462.2823; found: 462.2815.

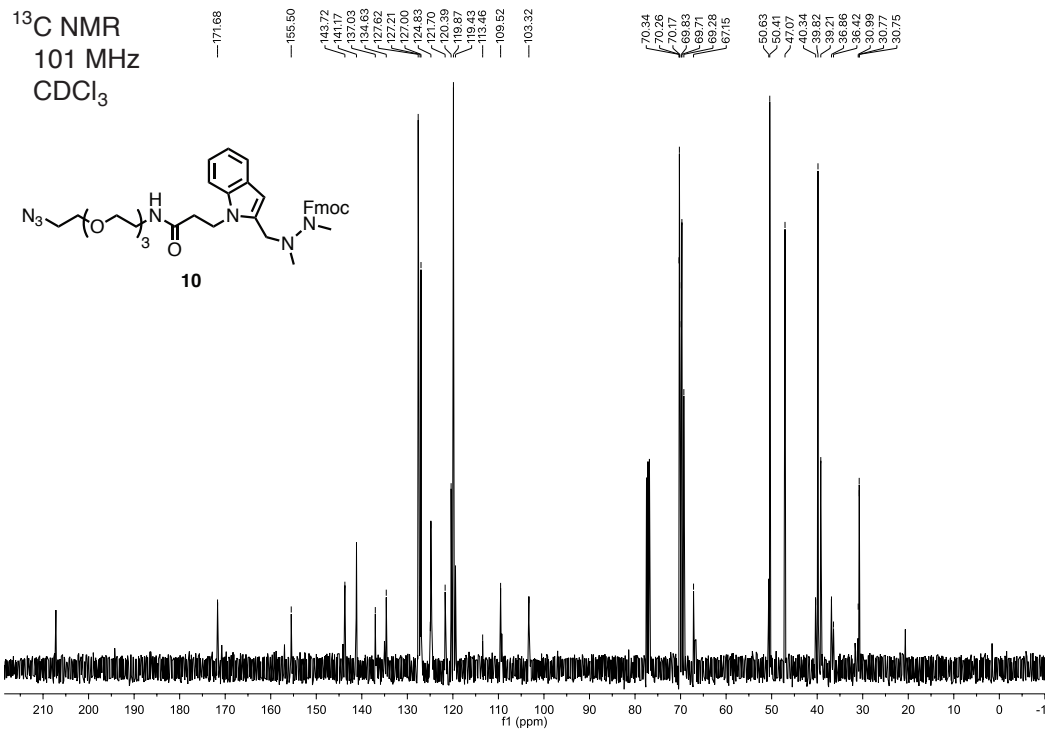
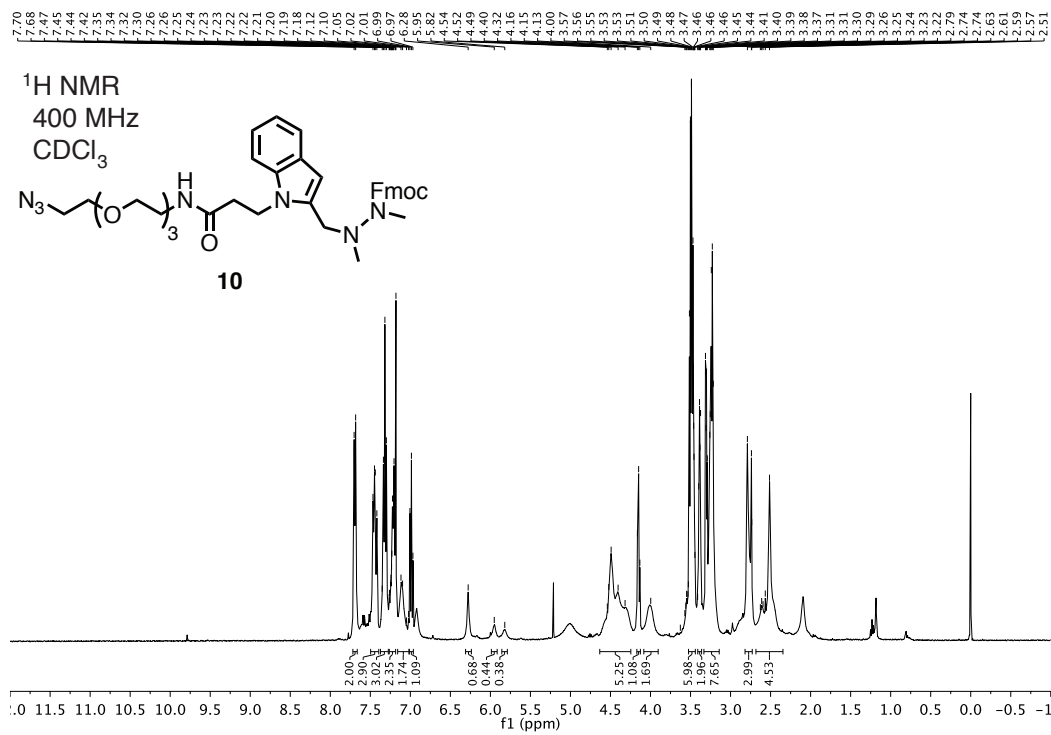


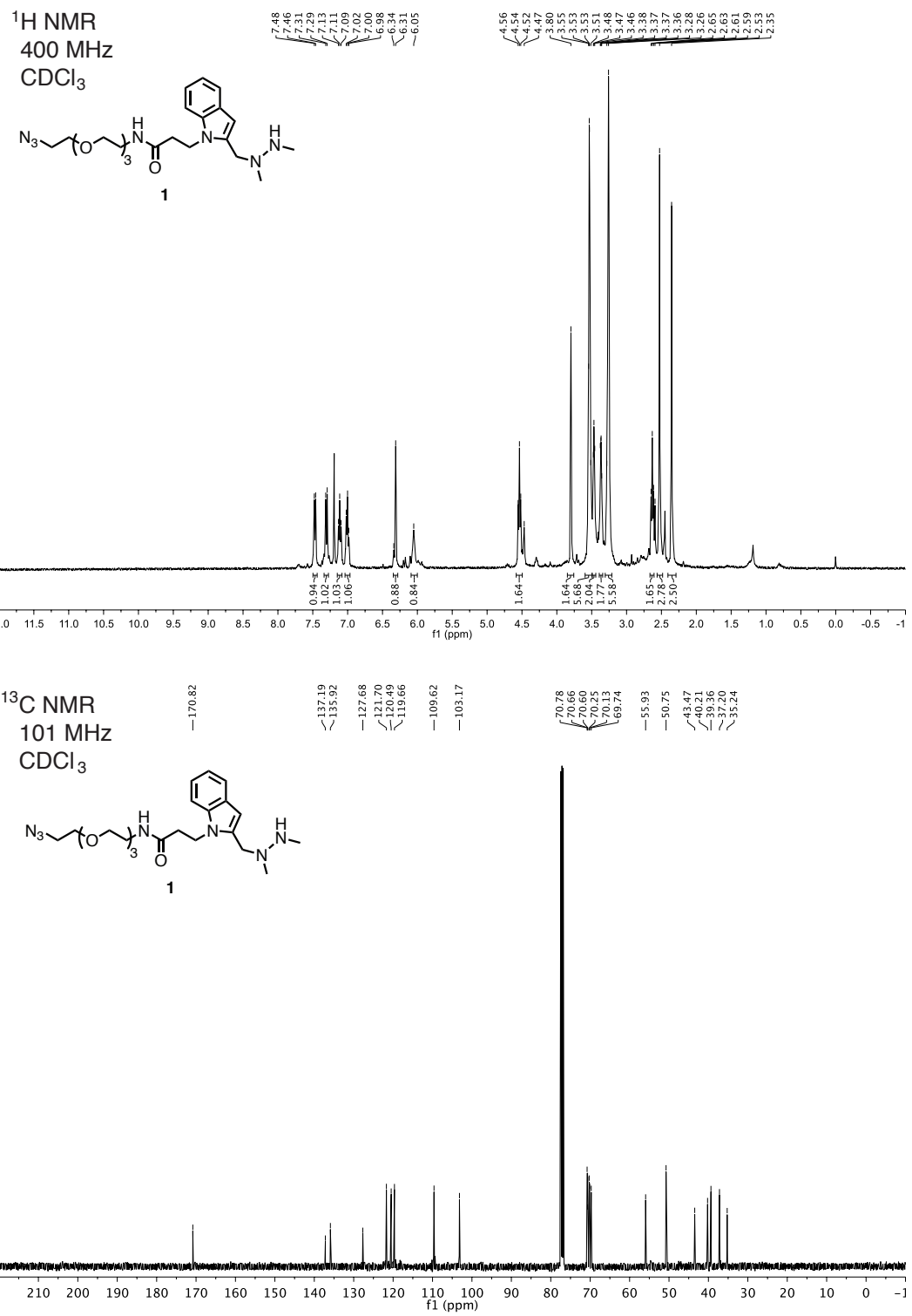
Synthesis of chloroacetamide-PEG4-DBCO

To a solution of chloroacetic acid (18.9 mg, 200 µmol, 1.2 equiv.) in DCM (189 µL) was added DBCO-PEG4-amine (87 mg, 167 µmol, 1 equiv.) in DCM (350 µL). The mixture was cooled in an ice bath to 0 °C and EDC (51.2 mg, 267 µM, 1.6 equiv.) in DCM (1 mL) was added. The mixture gradually came to RT and was stirred overnight. The mixture was concentrated in vacuo and then purified by flash chromatography on silica gel (0-10% MeOH in DCM) to give α -chloroacetamide-DBCO (**2**) as a yellow oil (77 mg, 77%), which was dissolved in DMSO and stored in aliquots at -80 °C. **TLC:**

(DCM:MeOH, 9:1 v/v) R_f = 0.4. **¹H NMR**: (400 MHz, CDCl₃) δ 7.66 (d, *J* = 7.4, 1H), 7.44–7.23 (m, 7H), 7.10 (br s, 1H), 6.54 (t, *J* = 5.6 Hz, 1H), 5.12 (d, *J* = 13.9 Hz, 1H), 4.03 (s, 2H), 3.71 – 3.54 (m, 15H), 3.52 – 3.45 (m, 4H), 3.36-3.21 (m, 2H), 2.55-2.44 (m, 1H), 2.35 – 2.26 (m, 2H), 2.03 – 1.86 (m, 1H). **¹³C NMR**: (101 MHz, CDCl₃) δ 172.1, 171.1, 166.2, 151.2, 148.2, 132.2, 129.2, 128.7, 128.5, 128.4, 127.9, 127.3, 125.7, 123.2, 122.6, 114.9, 107.9, 70.71, 70.68, 70.63, 70.48, 70.45, 70.3, 69.5, 67.2, 55.6, 42.8, 39.7, 37.0, 35.3, 34.9. **ESI-HRMS**: calc'd for C₃₁H₃₈CIN₃O₇ [M+H⁺]: 600.2476, found: 600.2466.

NMR Spectra





¹H NMR
400 MHz
CDCl₃

